

TOPICAL REVIEW

The discovery, development and future of GMR: The Nobel Prize 2007

Sarah M Thompson

Department of Physics, University of York, York, YO10 5DD, UK

Received 6 March 2008

Published 28 March 2008

Online at stacks.iop.org/JPhysD/41/093001**Abstract**

One hundred and one years after J J Thomson was awarded the Nobel Prize for the discovery of the electron, the 2007 Nobel Prize for Physics was awarded to Professors Peter Grünberg and Albert Fert for the discovery of giant magnetoresistance (GMR) in which the spin as well as the charge of the electron is manipulated and exploited in nanoscale magnetic materials. The journey to GMR started with Lord Kelvin who 150 years ago in 1857 made the first observations of anisotropic magnetoresistance and includes Sir Neville Mott who in 1936 realized that electric current in metals could be considered as two independent spin channels. Modern technology also has a significant role to play in the award of this Nobel Prize: GMR is only manifest in nanoscale materials, and the development of nanotechnology growth techniques was a necessary pre-requisite; further, the considerable demands of the magnetic data storage industry to drive up the data density stored on a hard disk fuelled an enormous international research effort following the initial discovery with the result that more than 5 billion GMR read heads have been manufactured since 1997, ubiquitous in hard disks today. This technology drive continues to inspire exploration of the spin current in the field now known as spintronics, generating new ideas and applications. This review explores the science underpinning GMR and spintronics, the different routes to its discovery taken by Professors Grünberg and Fert, the new science, materials and applications that the discovery has triggered and the considerable potential for the future.

1. Scientific background

It seems incredible that the first observations of magnetoresistance in a magnetic material were made 150 years ago by Lord Kelvin [1], 40 years before the electron was discovered by J J Thomson. Although the mechanisms responsible for anisotropic magnetoresistance (AMR) discovered by Kelvin and giant magnetoresistance (GMR) discovered by Grünberg [2] and Fert [3] are different, both are derived from the interaction of current carrying electrons and the magnetism of the host material. Magnetism in a ferromagnetic material arises from the spin-split band structure caused by a quantum mechanical exchange interaction between the electrons [4]. This results in a spin-polarized band structure in which there is an imbalance in the number of spin-up and spin-down electrons and consequently net magnetization, shown in figure 1. In AMR, the electron spin-orbit coupling results in a difference in the

scattering cross-section when the electron current is parallel or perpendicular to the magnetically aligned atoms [5]. This effect is significant, although only of the order of a few per cent. GMR however is based on spin-dependent scattering, first investigated in bulk ferromagnetic materials in the 1930s by, for example, Englert [6], Gerlach [7] and Potter [8], and considered theoretically by Sir Neville Mott in 1936 [9], whose work provided the foundation for Campbell and Fert in the 1960s and the 1970s to work on spin-dependent scattering [10, 11].

There are a number of crucial factors that lead to this spin dependent scattering in metallic ferromagnets—all of which derive from the spin-split band structure in a ferromagnetic material shown in figure 1. The first lies in the fact that these ferromagnets are transition metals, with a relatively high resistivity compared with noble metals—the reason for this resistivity, despite a similar conduction electron number density, is the availability of unoccupied states in the part-filled

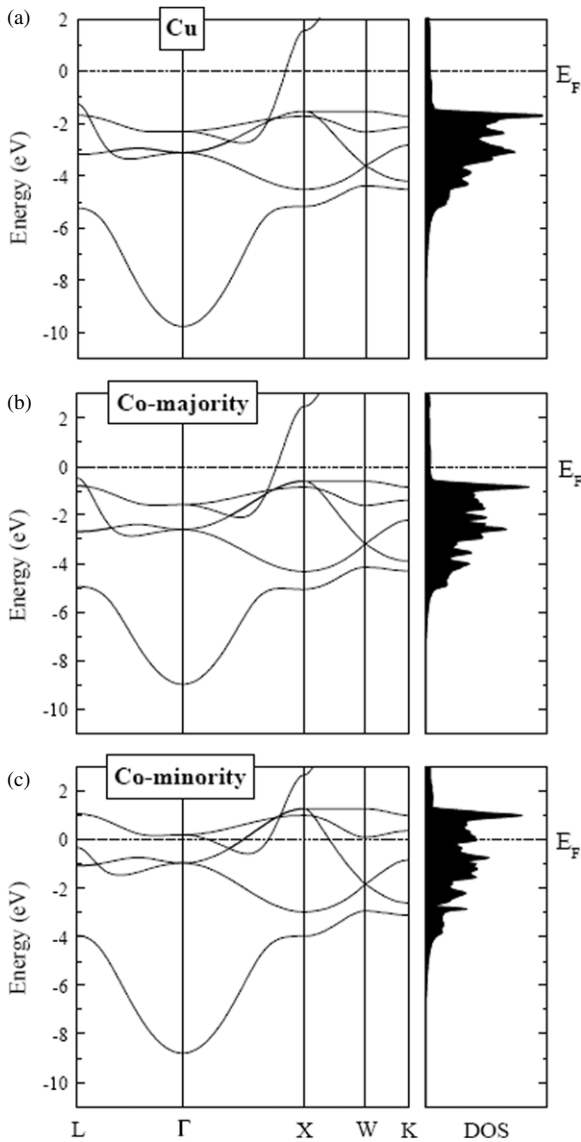


Figure 1. The electronic band structure (left) and density of states (right) for (a) non-magnetic Cu, (b) the majority spin electrons of fcc Co and (c) the minority spin electrons of fcc Co. The exchange-split d bands in the Co band structure are responsible for its ferromagnetic behaviour. The position of the Fermi level within the sp band of the majority electrons is responsible for their high conductivity in contrast to the minority electrons where the Fermi level lies within the d band resulting in low conductivity. (Reprinted with permission from figure 5 of [52]. Copyright 2001, Academic Press.)

d bands for scattering into, reducing the mean free path of the electrons. Secondly, it is these spin-split d bands that are responsible for ferromagnetism, resulting in a different density of states at the Fermi surface for spin-up and spin-down electrons and consequently a different scattering probability for spin-up and spin-down electrons. Usually, the scattering probability is greatest for the minority electrons. The final requirement for there to be little spin-flip scattering allowing the spin-up and spin-down conduction electrons to be considered as two independent current channels. From these basic ideas it is also possible to understand why similar effects are not observed in ferromagnetic rare earth metals, while

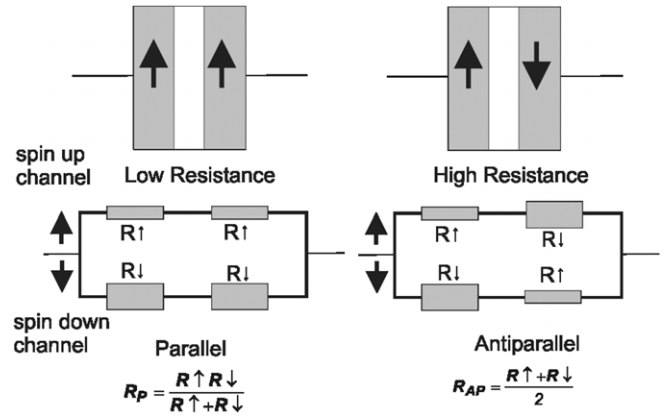


Figure 2. A schematic representation of GMR using a simple resistor network model. In the left picture, the spin-up channel is the majority spin channel in both the ferromagnetic layers, experiencing a low resistance ($R \uparrow$) throughout the structure. In the right-hand picture the spin-up channel is the majority spin channel ($R \uparrow$) in the first magnetic layer but the minority-spin channel ($R \downarrow$) in the second magnetic layer and vice versa for the spin-down channel. Neither spin channel is of low resistance throughout the structure and the overall resistance state of the structure is high. GMR occurs when the relative orientation of the magnetic layers is switched, usually by the application of a magnetic field.

although having a spin-split part-filled 4f band, it is well buried in the band structure and does not provide a significant scattering probability.

The combined effects of this spin-dependent scattering result in the spin filtering of the electron current when it passes through a ferromagnetic material, with the minority electrons experiencing more scattering. A GMR material exploits this spin-dependent scattering in a specially designed and fabricated structure. The simplest, a magnetic bilayer structure, can be modelled using a resistor network (figure 2 and equation (1)) in which the independent spin-up and spin-down electron current channels are represented by two parallel circuits and the resistance of the different layers represented by resistors:

$$\frac{\Delta R}{R} = \frac{R_{AP} - R_P}{R_P} = \frac{(R \downarrow - R \uparrow)^2}{4R \downarrow R \uparrow}. \quad (1)$$

In the first case, the magnetic layers are aligned parallel and the two spin channels experience quite different scattering. One of the electron channels will be the minority electron channel, experiencing significant scattering in both the layers, whereas the other channel will be majority electrons in both layers and will be much less scattered. Consequently the majority electron channel will dominate the conductivity in the parallel circuit and the combined structure will have a low total resistance. Conversely, in the second case, where the magnetic layers are antiparallel, both spin channels will in turn become majority or minority electrons as they travel through the different layers. Neither spin channel can therefore provide a low resistance path through the circuit and the combined resistance of the structure is consequently higher. GMR occurs when a magnetic structure is created which can be switched between the antiparallel and parallel alignment, thereby switching from a high to a low resistance state. The

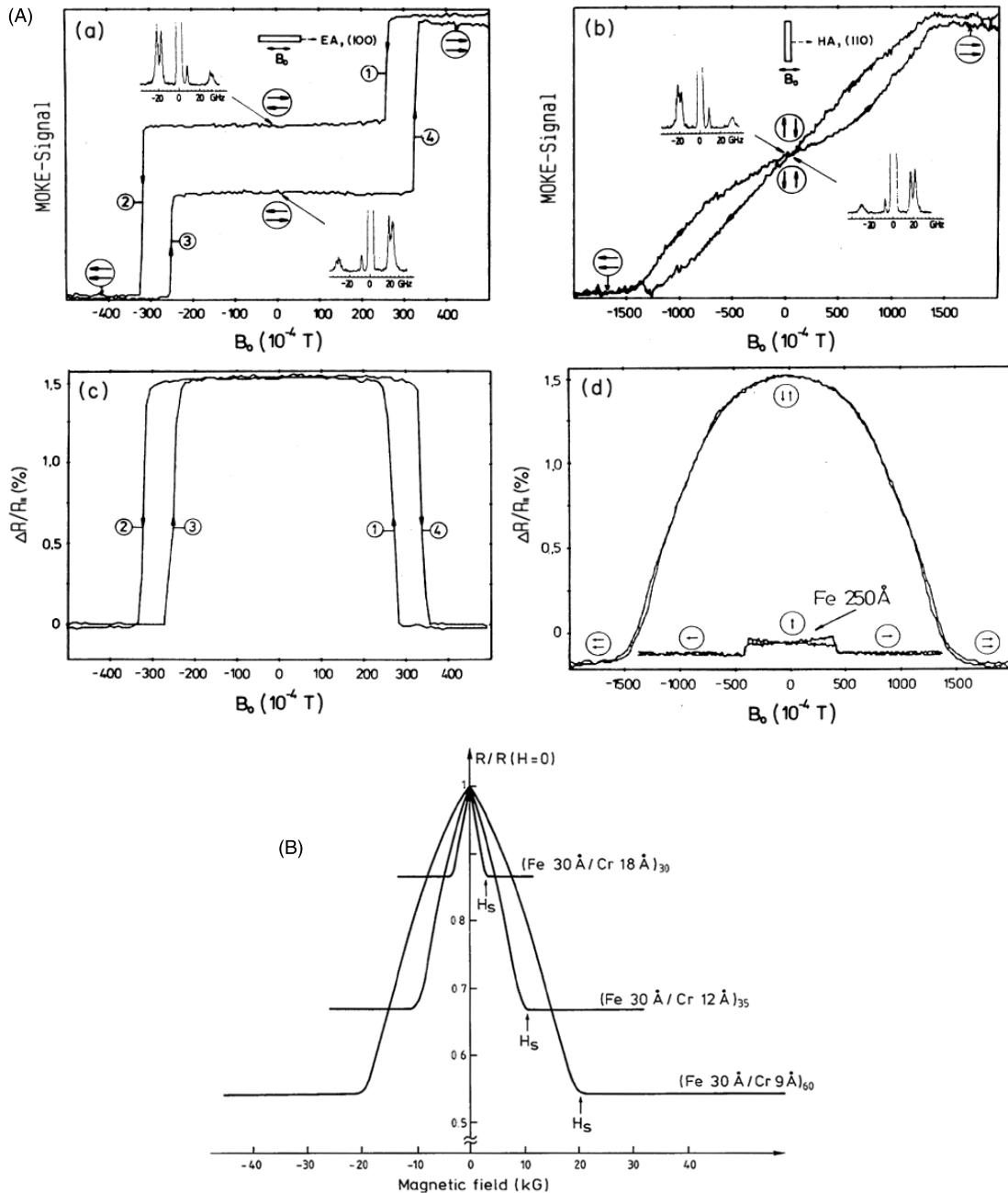


Figure 3. (A) The original measurement of GMR by the group of Peter Grünberg. The samples were Fe(12 nm)/Cr(1 nm)/Fe(12 nm) sandwiches deposited on GaAs (1 1 0) substrates by molecular beam epitaxy. The left and right panels show the results with the magnetic field applied along the easy and hard axes, respectively, in the plane of the multilayer. The upper graphs show the magnetization curves measured using the magneto-optic Kerr effect and the lower graphs the magnetoresistance measured with the current in the plane of the layers and at room temperature. The insets to the magnetization curve show the light scattering from spin waves signifying antiferromagnetic coupling. Graph (d) also shows the AMR measured on a 25 nm Fe film. (Reprinted with permission from figure 2 of [2]. Copyright 1989, American Physical Society.) (B) The original measurement of GMR by the group of Albert Fert. The graph shows the variation of electrical resistance with applied magnetic field for three Fe/Cr multilayers deposited by molecular beam epitaxy on GaAs (0 0 1) substrates and measured at a temperature of 4.2 K. The current and the applied magnetic field were applied in the plane of the layers and were parallel to each other along the [1 1 0] axis. (Reprinted with permission from figure 3 of [3]. Copyright 1988, American Physical Society.)

first independent observations of GMR by Grünberg [2] and Fert [3] were made on Fe/Cr/Fe trilayers and multilayers, respectively, reproduced in figure 3. In both figures, the change in resistance is plotted on the y-axis as the magnetic layers are gradually aligned in the applied magnetic field, plotted on the x-axis. Note that two different definitions of GMR are in common use, and in fact both were used in these original

reports. In the Fert graph the change in resistance is divided by the resistance in the antiparallel state (zero applied field), and in the Grünberg case, the change in resistance is divided by the resistance in the parallel alignment (high applied field) case. The larger effect observed in the Fert experiments is due to the multilayered structure and the lower measurement temperature of 4.2 K.

2. The journey to the Nobel Prize

In 1998 at the International Conference of Magnetic Films and Surfaces (ICMFS) held in Le Creusot (France), both Peter Grünberg and Albert Fert gave presentations on the large magnetoresistance they had observed in Fe/Cr/Fe layered systems and after discussing their results realized they were observing the same effect.

2.1. Peter Grünberg's journey to the Nobel Prize

Peter Grünberg initially specialized in optical spectroscopy and rare earth materials. Following his PhD studies in Darmstadt (Germany) and a postdoctoral fellowship in Ottawa (Canada), in 1972 he joined the recently founded Institute of Magnetism in Jülich (Germany) to study bulk and surface spin waves in the rare earth based magnetic semiconductors EuO and EuS. Inspired by new developments in optical techniques, and opportunities for building new equipment in a new institute, he developed a multipass Fabry–Perot interferometer which employed light scattering to investigate collective excitations. Having succeeded in making the first observations of the Damon–Esbach surface mode in EuO by light scattering, the group went on to study coupled Damon–Esbach spin waves in bilayers of ferromagnetic materials separated by a thin, non-magnetic metallic layer. Using the Landau–Lifshitz equation, they predicted the form of optical modes in the cases where the Fe layers would be oriented parallel (ferromagnetic coupling) and antiparallel (antiferromagnetic coupling) and successfully observed the ferromagnetic case. However, at that time the only known forms of magnetic coupling both resulted in ferromagnetic order. They were pin-hole coupling, caused by direct magnetic bridges formed through compromised interlayers, and Néel coupling resulting from the effect of the stray magnetic field from one ferromagnetic layer on the other. Realizing that Fabry–Perot interferometry could distinguish between these different types of coupling, they began an investigation of coupling in ferromagnetic bilayers. Whilst studying the variation in coupling as a function of interlayer thickness in the Fe/Cr/Fe system, they observed the predicted signature of antiparallel layer orientation and thereby discovered synthetic antiferromagnetic exchange coupling [12]. At the same time, similar discoveries of antiferromagnetic exchange coupling were made in the rare earth multilayer structures of Gd/Y [13] and Dy/Y [14]. It was eventually realized that in all these cases, exchange coupling is an extension of the Ruderman–Kittler–Kasuya–Yosida [15] coupling responsible for magnetic order within magnetic rare earths. This originates from spin polarization induced in the interlayer by the ferromagnetic layer setting up a spin-density wave. The relative orientation of the layers will depend on multiple quantum interference effects [16] of the electrons reflecting from internal interfaces, resulting in an oscillatory coupling as clearly demonstrated by Parkin [17] and illustrated in figure 4. This was further very visually illustrated using a variety of experimental techniques such as Brillouin light scattering [18, 19], the magneto-optic Kerr (MOKE) effect and scanning electron microscopy with polarization analysis [20].

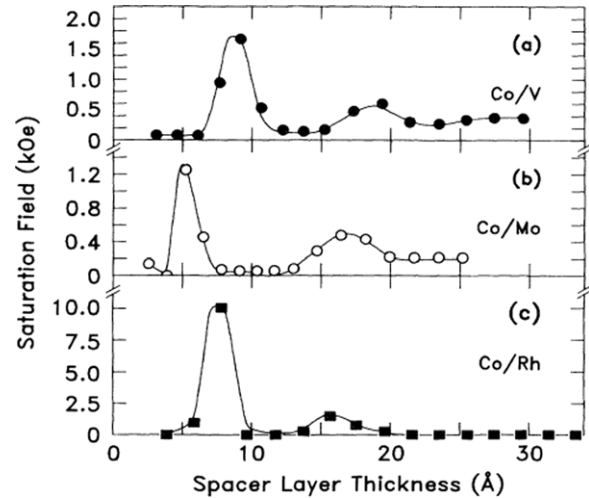


Figure 4. The oscillation of exchange coupling between Co layers across different spacer layers determined by the magnetic field required to reach 80% of the saturation magnetic moment. Note the period of oscillation of the coupling from ferromagnetic (low saturation field) to antiferromagnetic (high saturation field) is similar at about 1 nm for all the elements presented. This was part of an extensive study of many different ferromagnetic and spacer layers by Parkin [17]. (Reprinted with permission from figure 2 of [17]. Copyright 1991, American Physical Society.)

In a phenomenal series of experiments, Parkin investigated the dependence of coupling on different ferromagnetic and non-magnetic layers showing that to a reasonable approximation the oscillation period of about 1 nm is common to most material combinations [17, 21], figure 4.

Having established antiferromagnetic exchange coupling, Grünberg, looking for other material properties that could be studied in these new magnetic multilayers, turned to electrical magnetotransport studies, resulting in his discovery of GMR in 1988 as shown in figure 3 [2]. They also used their light scattering technique to show the correlation between the coupling state of the ferromagnetic layers and the electrical resistance of the structure; the coupling peaks can be seen in the insets of figure 3(A). Realizing the potential for exploiting this magnetoresistance effect as a commercially useful magnetic sensor, he filed a patent in April 1988 [22].

2.2. Albert Fert's journey to the Nobel Prize

Albert Fert began his research on spin-dependent scattering during his PhD. Stimulated by Mott's theoretical ideas of the two-spin-current model from the 1930s [9], he and Ian Campbell exhaustively studied spin-dependent scattering in ferromagnetic metals, and in particular spin-dependent impurity scattering [10, 11]. They proved that spin-down and spin-up electrons behave as two independent spin-dependent current carrying channels and determined different spin-scattering asymmetries for a wide range of different impurities. They proposed a variety of different ternary alloy structures, in which by doping Ni with mixed impurities with different spin asymmetries a different spin-dependent scattering would result [23]. These ideas were a clear pre-cursor to GMR, but the next steps required the creation of nanoscale metallic thin

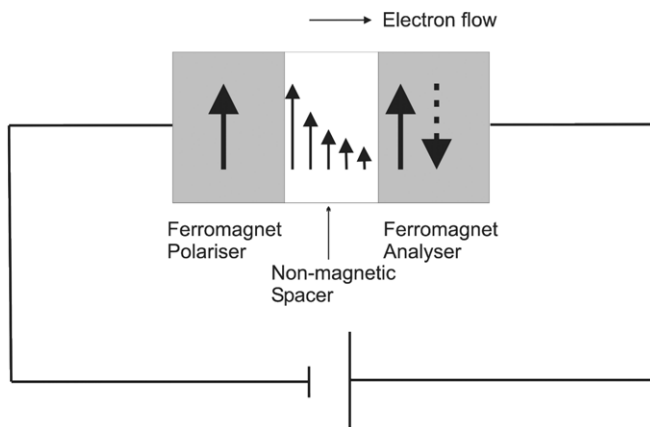


Figure 5. The principal constituents of a GMR or spintronic device. The current is first spin polarized by a ferromagnetic material, indicated by the upwards arrow, and then injected into a non-magnetic spacer layer. The spin orientation in the spacer layer will decay due to spin-flip scattering over the length scale of the spin-diffusion length, and it is important that this spin memory is retained by the time the electrons reach the second ferromagnetic layer, or analyser.

films—the growth of which was very much in its infancy at the time.

As thin film growth technology, especially molecular beam epitaxy, improved to the point where nanoscale magnetic thin films and multilayers could be grown with great precision, the opportunities for designing magnetic materials became an experimental reality. When Grünberg published his paper in 1986 on antiferromagnetic coupling in Fe/Cr/Fe layers [12], Fert realized that at last he could design and test structures that might exhibit interesting spin-dependent scattering effects—and thus he discovered GMR in Fe/Cr/Fe multilayers as shown in figure 3(B) [3].

3. Different GMR geometries and structures

Although the discovery of GMR was made in antiferromagnetically coupled magnetic multilayers—this sample structure is not a pre-requisite for the effect. The crucial factors are that the current carrying electrons must be spin polarized by a ferromagnetic material, that this spin polarized current pass through at least one other ferromagnetic material where its scattering is determined by the local magnetic orientation (spin detection) and finally that the spin-polarized current must retain its spin whilst travelling between the two magnetic regions. The spin-diffusion length, l_{sf} , characterizes the distance over which this spin memory decays. Further, the relative magnetic orientation of the ferromagnetic polariser and detector must be altered by the application of a magnetic field. These major features of a GMR device are schematically illustrated in figure 5.

3.1. Domain wall resistance and nanoconstrictions

We should first ask why GMR is not routinely observed in any ferromagnet with a magnetic domain structure with the different ‘layers’ corresponding to magnetic domains. A ‘GMR’ effect might then be observed as the magnetic

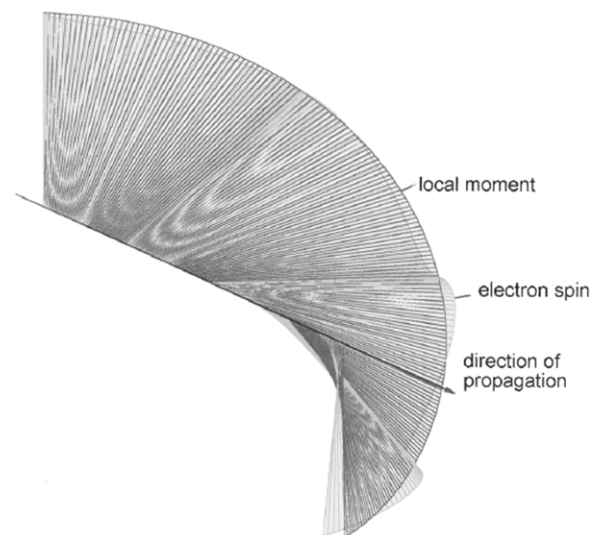


Figure 6. Numerical simulations of the orientation of the electron spin as it traverses a domain wall and attempts to track the rotation of the local electron spin. The results show that by the time the electron reaches the edges of the domain wall, there is a small offset between its orientation and the local spin orientation. This offset is larger for a narrower domain wall. (Reprinted with permission from figure 3 of [25]. Copyright 1996, American Physical Society.)

domains are aligned with an applied magnetic field. However, magnetic domains are separated by domain walls, within which the magnetic orientation of the magnetic atoms rotates [4]. Depending on the magnetic properties of the material, such as the strength of the exchange energy and the local magnetic anisotropy, the domain wall width can be relatively wide, typically 40nm for bulk Fe. If the orientation of the spin of the current carrying electrons is able to follow this local moment rotation, they will remain majority electrons throughout, thus preventing any GMR-like effects occurring. The presence of a nanoscale non-magnetic interlayer in a magnetic multilayer structure removes the domain wall and allows a rapid switch in local moment orientation which results in GMR.

However, with careful control over the dimensions of the domain wall, it is possible to investigate the magnetoresistance through a domain wall. This normally means restraining the domain wall, for example, in a thin film with perpendicular anisotropy or in a carefully designed nanostructure. An excellent review of this topic is given by Marrows [24]. In the diffusive regime, there is now reasonable consensus that the prime reason for domain wall magnetoresistance is the mistracking of the electron spin as it traverses the domain wall as described above and illustrated in figure 6 [25], Levy and Zhang [26], Gregg [27].

By constraining the domain wall still further, for example, by creating a nanocontact between lithographically created nanowires, it is possible to enter a ballistic regime where conductance is affected by the availability or otherwise of quantum conduction channels which can be highly spin-polarized. This research area of ballistic magnetoresistance (BMR) was triggered by Garcia *et al* [28] in 1999, who reported a magnetoresistance of 280% in Ni nanocontacts in applied fields of only 120Oe at room

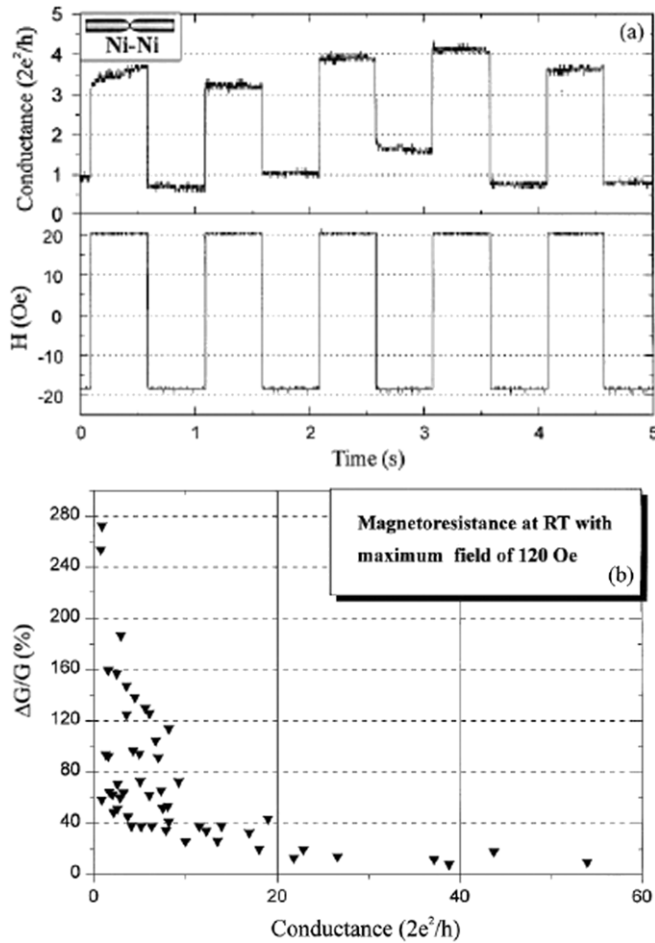


Figure 7. (a) Room temperature magnetoresistance measurements on Ni–Ni nanoconstrictions formed from two Ni wires of milli metre radius, (b) shows the dependence of the magnetoresistance measured at 120 Oe as a function of conductance, indicating a larger effect for smaller conductance values. (Reprinted with permission from figure 2 of [28]. Copyright 1999, American Physical Society.)

temperature (shown in figure 7), and treated theoretically by Bruno [29]. However, there remains much debate about the detailed mechanisms responsible—partly due to the difficulties in deconvoluting the various effects experimentally [24].

3.2. Magnetic multilayers and spin-valves

In order to appreciate the impact of the device structure on the GMR some consideration must be given to the electron scattering mechanisms and where they take place. Scattering processes may be elastic or inelastic and may or may not result in momentum change or spin flipping [30]. Consequently, they will affect in different ways the electron mean free path, the diffusion constant or the spin–flip scattering time. Importantly, scattering will also occur at the surfaces and interfaces of the material as well as within the bulk. The different length scales that result from these processes determine the GMR behaviour of the device.

The electrons must travel through the entire structure whilst maintaining their original spin orientation in order for them to experience spin-dependent scattering in the different layers. For multilayer structures where the net electron current

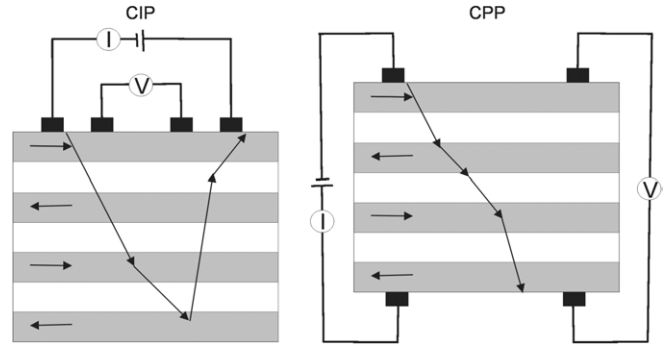


Figure 8. Schematic diagram of the principal two geometries of GMR. In the first picture the net current direction is in the plane of the layers and it is important that the mean free path of the electrons is longer than the sum of the layer thicknesses so that the electrons sample the different layers. In the second picture, the net current direction is perpendicular to the layers and the critical length scale becomes the spin-diffusion length.

direction is in the plane of the layers (current in the plane or CIP geometry), this means that the electron mean free path (typically only tens of nanometres) should be longer than the total thickness of the multilayer structure as indicated in figure 8. Where contacts are made to the top and bottom of the structure and the net current direction is perpendicular to the layers (current perpendicular to the plane or CPP geometry, figure 8) [32] the critical length scale is usually the spin-diffusion length which is related to the mean free path as

$$l_{sf} \approx \sqrt{\frac{v_F \tau_{sf} \lambda}{3}}, \quad (2)$$

where v_F is the Fermi velocity, τ_{sf} is the spin–flip relaxation time and λ the electron mean free path.

The discovery of antiferromagnetic coupling was critical to the discovery of GMR, providing as it did antiparallel alignment of the magnetic layers which could be overcome by an applied magnetic field. However, antiferromagnetic coupling itself is not a prerequisite for GMR. In fact the strength of antiferromagnetic coupling proved to be a problem in the development of GMR materials for magnetic sensors as a considerable magnetic field is often required to overcome the coupling exchange energy. A different way of achieving antiparallel alignment, which could easily be removed with the application of a magnetic field, was therefore sought and extremely successfully implemented by researchers at IBM. The new multilayer structures [31, 33–35], called spin-valves, typically consist of a ferromagnetic layer pinned by direct exchange coupling to an antiferromagnetic layer and separated by a decoupling non-magnetic layer from an unpinned and magnetically soft ‘free’ ferromagnetic layer, easily switched by a small applied magnetic field (illustrated in figures 9 and 17). It is also possible to achieve similar effects by creating magnetic multilayers with alternating soft and hard magnetic materials such that there are parts of the hysteresis curve where there is antiparallel alignment of the layers [36].

In the early 1990s, there was considerable debate on the location of spin-dependent scattering: did it originate within the ‘bulk’ of the thin film or was it dominated by interfacial

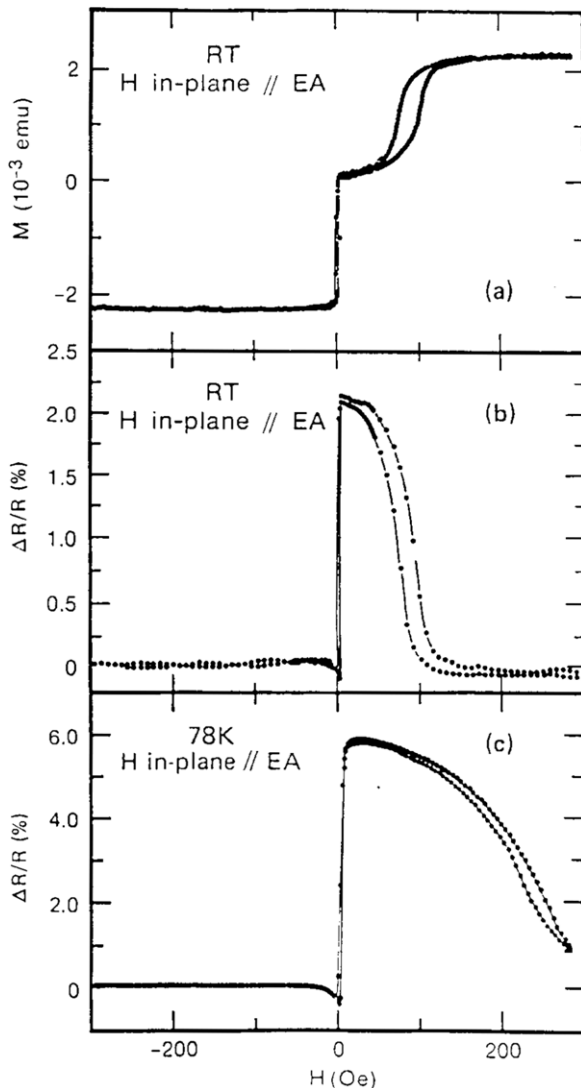


Figure 9. Typical magnetic and magnetoresistive behaviour of a spin-valve with structure: Si/NiFe(15 nm)/Cu(2.6 nm)/NiFe(15 nm)/FeMn(1 nm)/Ag(2 nm). The bottom NiFe layer is free to rotate in a small magnetic field, whereas the upper NiFe layer is pinned to the antiferromagnetic FeMn layer by exchange biasing until much higher magnetic fields are applied. This results in a rapid switching between parallel and antiparallel alignment and consequently low and high electrical resistance in small applied magnetic fields. The magnetic field is applied along the easy axis antiparallel to the exchange field created by the FeMn layer. (Reprinted with permission from figure 1 of [31]. Copyright 1991, Elsevier.)

scattering. The answers determine the optimum structure for the multilayer. In general, spin-independent scattering is detrimental to GMR—reducing the electron mean free path and the spin-diffusion length without contributing any spin-dependent effects. Such scattering often results from the microstructure such as vacancies, defects, roughness and dislocations. These can often be relieved by careful growth or materials processing, by annealing for example. However, scattering within the ferromagnet or at an interface may be spin dependent, thereby making a positive contribution to GMR. This importance of interfacial scattering was very nicely demonstrated in a set of experiments by Parkin in which a

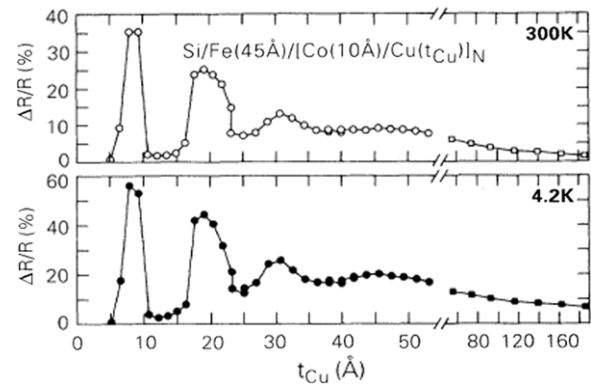


Figure 10. The variation of maximum magnetoresistance due to the change in exchange coupling as it varies with interlayer thickness in Co/Cu based multilayers showing the very large values that can be obtained at the first antiferromagnetic coupling peak. The multilayers were sputtered at IBM onto Si substrates with an Fe underlayer: Si/Fe(4.5 nm)/[Co(1 nm)/Cu(t_{Cu} nm)] N where t_{Cu} varies from 0.5 to 18 nm and N is 16 for $t_{Cu} < 5.5$ nm and 8 for $t_{Cu} \geq 5.5$ nm. In all cases the top Cu layer was extended to form a 5.5 nm capping layer. (Reprinted with permission from figure 3 of [38]. Copyright 1991, American Physical Society.)

variable thickness, very thin, layer of various ferromagnetic materials was inserted at the interface of ferromagnet/non-magnetic/ferromagnetic sandwiches [37]. Spin-dependent scattering arises from the band structure, for example, if there is a matching of the electronic potentials in one spin direction and not in the other. This can also occur at an interface or at impurity sites where there is band matching between two elements, for example, in the Fe/Cr system there is good band matching for the spin-down band, but poor matching for the spin-up band. The reverse situation occurs for the case of Ni or Co interfaced with Cu where it is the spin-up band of the ferromagnet that is full, as can be seen from the Co and Cu band structures illustrated in figure 1.

The Co/Cu system is a particularly good system for GMR as there is also good lattice matching resulting in low dislocation density at the interface and consequently low spin-independent scattering. The high values of GMR possible in Co/Cu coupled multilayers at room temperature was demonstrated by Parkin *et al* [38] and illustrated in figure 10. Reference [39] in particular presented room temperature GMR values in excess of 65% in Co/Cu multilayers where Fe buffer layers were used to produce layers with a very high degree of structural integrity. Interdiffusion at interfaces where the elements are miscible can complicate the situation further; alloying will change the band structure and consequently affect the scattering and also the magnetic behaviour. Often the Curie temperature is altered, for example, in Ni/Cu or Co/Cr, rendering the alloy non-magnetic at room temperature with significant consequences for both the spin-dependent nature of the scattering and the interlayer exchange coupling [40]. Detailed (and difficult) band structure calculations are necessary to predict the exact spin-dependent behaviour of a particular material combination at the interface [41, 42].

There is ongoing effort to develop better ferromagnetic material combinations to increase spin-dependent scattering. One candidate group of materials are half-metals which have

their majority-spin band entirely below the Fermi level and so have an insulating majority band, but a metallic minority band [43]. These materials should in theory provide 100% spin polarization. However, it is often the case that at the critical ferromagnetic/non-magnetic interface, the disrupted structure destroys the half-metallic behaviour. Progress is however being made, for example by Hwang and Cheong who measured an enhanced magnetoresistance in a CrO₂ based structure [44].

Spin valves, uncomplicated by the presence of interlayer exchange coupling, provided an ideal structure for the study of both the source of the scattering and the impact of the layer thicknesses on the resulting GMR. These studies were comprehensively reported in a review by Diény in 1994 [34].

The thickness of the non-magnetic layer primarily affects the interlayer exchange coupling—either to decouple the layers in a spin-valve or to achieve the desired interlayer coupling energy in a coupled system. Increasing the thickness of the non-magnetic layer beyond what is required by these coupling considerations is usually detrimental to the GMR: typically the non-magnetic material has a higher conductivity than the ferromagnetic material and therefore has the potential to act as an electrical shunt. This effect must also be taken into account when deciding on a capping material for the structure. In addition, some non-magnetic materials, such as Au, have strong spin-orbit coupling and thus reduce the spin-diffusion length of the structure. These effects can be described by the following phenomenological equation [35]:

$$\frac{\Delta R}{R}(t_{\text{NM}}) = \left(\frac{\Delta R}{R}\right)_1 \left[\exp\left(-\frac{t_{\text{NM}}}{l_{\text{NM}}}\right) / \left(1 + \frac{t_{\text{NM}}}{t_0}\right) \right], \quad (3)$$

where t_{NM} is the thickness of the non-magnetic layer, l_{NM} is the mean free path of the electrons in the non-magnetic layer, t_0 is the effective thickness of the rest of the multilayer causing shunting of the electrical current and $(\Delta R/R)_1$ is a normalization coefficient. In all cases, however, care must be taken that the non-magnetic layer is continuous, preventing direct magnetic pin-hole coupling which would result in ferromagnetic alignment of the magnetic layers.

The GMR of a spin-valve typically increases with the thickness of the free ferromagnetic layer (t_{F}) to a maximum ($t_{\text{F}} < 10 \text{ nm}$) and then slowly decays. This is shown for three different ferromagnetic materials in figure 11 [34]. The position of the maximum arises from a number of different effects. The magnetic layers must be thick enough to provide sufficient bulk spin-dependent scattering: in practice this means that t_{F} must be longer than the mean free path of the spin-down electrons. Figure 11 reveals the differences that result from the relative importance of bulk versus. interfacial spin-dependent scattering in the material. For permalloy (Ni₈₀Fe₂₀), for which bulk spin-dependent scattering is important, the maximum t_{F} is greater than in the case of Fe for which there is very little bulk spin-dependent scattering. The minimum t_{F} required for interfacial scattering is determined by the thickness required to create a ‘bulk-like’ electronic band structure for the ferromagnetic material at the interface. In ferromagnetic bilayer (or sandwich) structures, such as those initially studied by Grünberg, surface scattering

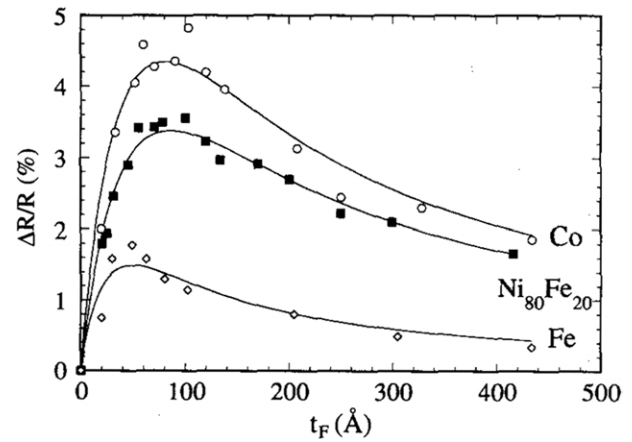


Figure 11. The room temperature variation of maximum magnetoresistance with the thickness of the free ferromagnetic layer for a series of three sputtered spin-valves with structure: Si/TM/Cu(2.2 nm)/NiFe(4.7 nm)/FeMn(7.8 nm)/Cu(1.5) where TM is the ferromagnet Fe, NiFe or Co. (Reprinted with permission from figure 5(b) of [34]. Copyright 1994, Elsevier.)

starts to become significant, and t_{F} must now be longer than the mean free path of the spin-up electrons.

As t_{F} is increased beyond its optimum value, then the ferromagnetic layer itself will also act as an electrical shunt and so the GMR will decrease. This effect is more significant in a multilayer structure for which the number of interfaces sampled by the current carrying electrons will reduce as the overall thickness of the structure exceeds the electron mean free path. The dependence of the GMR on the thickness of the ferromagnetic layer is reasonably well described by the following expression [45]:

$$\frac{\Delta R}{R}(t_{\text{F}}) = \left(\frac{\Delta R}{R}\right)_0 \left[1 - \exp\left(-\frac{t_{\text{F}}}{l_{\text{F}}}\right) / \left(1 + \frac{t_{\text{F}}}{t_0}\right) \right], \quad (4)$$

where t_{F} is the thickness of the ferromagnetic layer, l_{F} is the mean free path of the electrons in the ferromagnetic layer (see [34] for a discussion of which spin channel dominates the behaviour), t_0 is the effective thickness of the rest of the multilayers causing shunting of the electrical current and $(\Delta R/R)_0$ is a normalization coefficient.

The impressive control that modern growth technology allows enables a GMR structure to be designed taking into account all these different parameters thus optimizing the response for a particular application. For example, an effective way of benefiting from the soft magnetic properties of Ni₈₀Fe₂₀, avoiding the problems of interdiffusion at the interface with Cu and exploit the effective spin-dependent scattering at the Co/Cu interface is to construct a Ni₈₀Fe₂₀/Cu multilayer with a thin layer of Co ‘dusting’ the interface [37].

3.3. Granular GMR materials

Provided the basic criteria for GMR are satisfied, the layering of the different materials is not required. This was first demonstrated in 1992 by Berkowitz *et al* [46] and Xiao *et al* [47] both of whom created GMR single film materials from heterogeneous alloys in which single domain ferromagnetic

particles are embedded in a non-magnetic matrix. The attraction of these materials is that they can be very easily manufactured, provided the ferromagnetic and non-magnetic materials are immiscible, using techniques such as co-deposition—or even mechanical alloying to produce a bulk material with a nanoscale microstructure [48]. The critical length scales in granular systems are the particle diameter, analogous to the thickness of the ferromagnetic layer, and the inter-particle separation, analogous to the thickness of the non-magnetic layer. The particles must also be small enough to be single domain. A comprehensive theory of the GMR in granular systems is given by Zhang and Levy [49, 50]. The GMR in granular systems is especially sensitive to the magnetization process and in particular to any interactions between the particles—so much so that the GMR can be used as a sensitive probe of the magnetic correlations between the particles [51].

4. Theories of GMR

As GMR arises from the detailed properties of the electronic band structure of both the ferromagnetic and non-magnetic elements, there is clearly good reason to develop a full quantum mechanical treatment of GMR. However, a great deal of physical insight can be gained from a semi-classical treatment of GMR. In particular, quantum mechanical models can be used to treat the scattering and then employed within the classical dynamics of electron transport theory using the Boltzmann equation. Which model is appropriate depends on the dominant critical length scale for the particular structure. If the total structure is thinner than the mean free path of both spin channels, then the simple resistor model, equation (1), can be employed—however this condition is rarely met. An excellent review of the various theoretical approaches to modelling GMR is given by Tsymbol [52].

The first semi-classical free-electron model of the GMR was developed by Bob Camley from the USA and Josef Barnaś from Poland who were visiting Peter Grünberg in Jülich in the late 1990s [53, 54]. They successfully used the Boltzmann transport equation to describe the GMR in CIP structures and by using the Fuchs and Sondheimer formulation they were able to take into account the finite thickness of the films and consider reflection, transmission and diffusive scattering at the surface and interfaces and also incorporate spin-dependent mean free paths. By fitting to the experimental data they determined a number of key parameters. In particular they identified diffusive scattering at the interfaces to be the primary mechanism for the GMR in the Fe/Cr/Fe system, deducing that there was more than a five-fold difference in the scattering of the spin-up and spin-down electrons. In contrast, in $\text{Ni}_{80}\text{Fe}_{20}$, spin-dependent scattering within the ferromagnetic layer was found to dominate. In these early models, the additional presence of AMR was ignored, leading to some deviations between the theory and the experiment. The model qualitatively accounts for many of the features and trends of GMR, although caution must be taken in attempting to extract quantitative parameters. In the CIP geometry, the current and the magnetic field can be assumed to be uniform in the direction

of the transport which is the plane of the multilayer. The situation is more complex in the CPP geometry where the net transport direction is perpendicular to the plane of layers and along which the structure is non-uniform.

In 1993 Thierry Valet and Albert Fert published a semi-classical model for use in the CPP geometry, using the Boltzmann equation also but with the addition of spin-dependent electrochemical potentials [55]. The ideas of spin accumulation proved to be particularly applicable for the CPP geometry, and then later for the consideration of spin injection in spintronic materials. In a CPP structure, the spin-filtered current is injected into a non-magnetic material transferring with it spin-angular momentum and creating spin accumulation. The size of the spin accumulation is determined by the rate at which the spins are injected and their decay by spin-flip processes as they move away from the interface. The spin-diffusion length, l_{sf} , characterizes the distance over which this spin accumulation exponentially decays away from the interface as $n = n_0 e^{-x/l_{sf}}$, where n is the spin-electron density at a distance x away from the interface and n_0 is the electron spin density at the interface. In the Valet and Fert model, the assumption is made that the spin-diffusion length is much longer than the electron mean free path, and the electrochemical potentials of the two spin channels are treated independently. They showed that if the mean free path is shorter than the spin-diffusion length, a macroscopic model can be used. Johnson and Silsbee [56, 57] and van Son *et al* [58] had already developed such a macroscopic model for the interface resistance and extended it to multilayers by summing the interface resistances in series [59]. Valet and Fert demonstrated that it is necessary to take into account the overlapping spin accumulations at successive interfaces to correctly model the CPP-GMR. This model also provided an invaluable tool with which to separate the effects of bulk and interface scattering [60].

As the film thickness becomes comparable to the mean free path, quantum mechanical effects become increasingly important, leading to the discretization of energy levels. The critical parameter is when the energy splitting of the subband becomes comparable to the lifetime broadening due to scattering—a condition that becomes more likely when a realistic defect density is considered. In general both semi-classical and quantum free-electron models can be made to fit experimental data although they give quantitatively different results. A full spin-polarized band structure is needed to make quantitative predictions.

The first quantum free-electron model was created by Levy *et al* [61, 62], modelling the electron transport, as with many other researchers, using the Kubo linear response theorem. In momentum space, they modelled the scattering of the electrons due to random-point scatterers using a spin-dependent scattering potential which contained both spin-dependent and spin-independent components. Different values could be assigned at different points in the structure such as the interface and the bulk and could be adjusted for different material combinations. This was a useful model and can be shown to reduce to the resistor model in the CIP geometry when the mean free path is greater than the layer

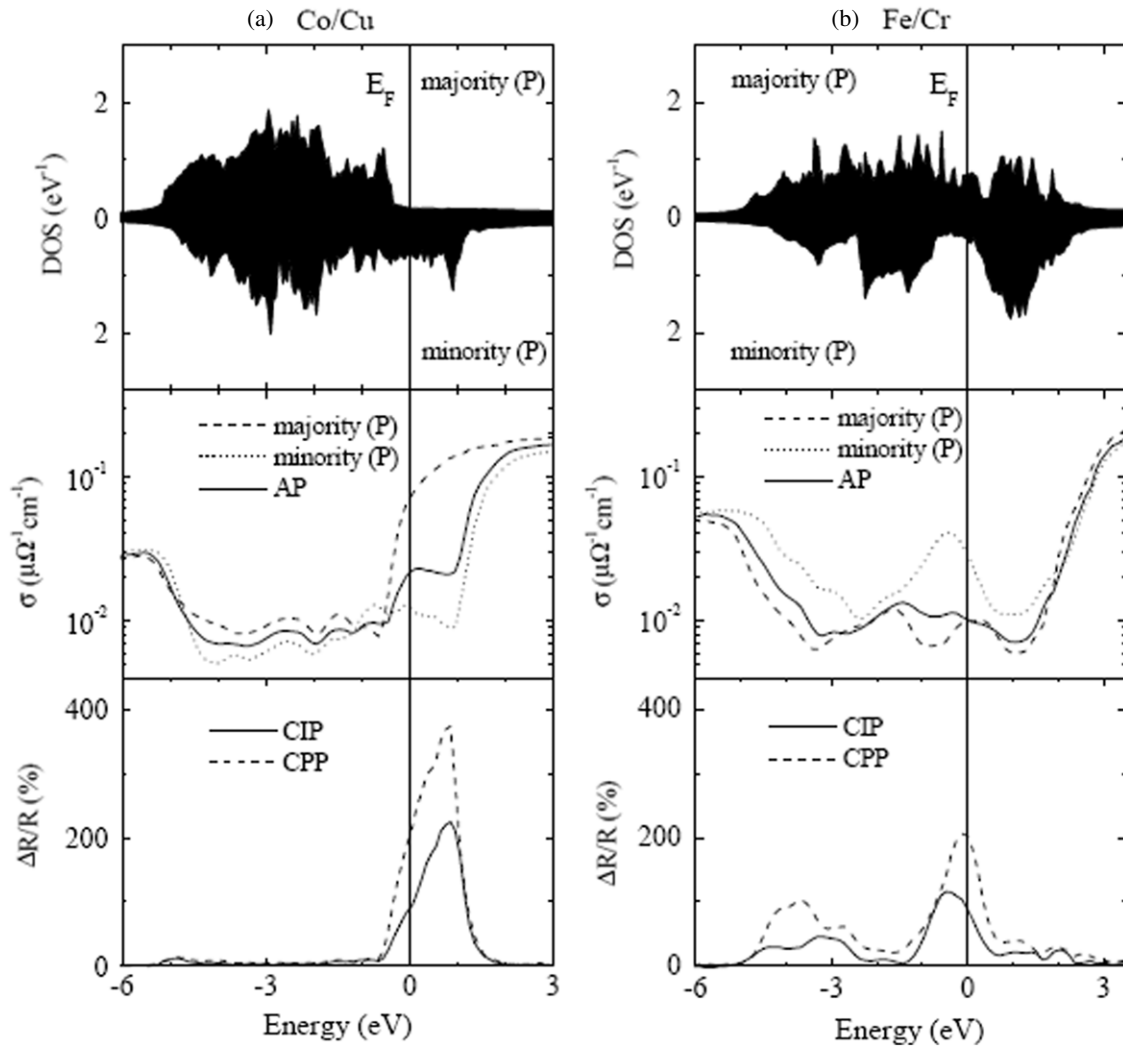


Figure 12. The Tsymbal and Pettifor tight-binding model of GMR [75–78]: the density of states, conductivity and GMR in both the CIP and CPP configurations of Co_4/Cu_4 and Fe_4/Cr_4 multilayers plotted as a function of electron energy. (Reprinted with permission from figures 1 and 2 of [75]. Copyright 1996, IOP Publishing.)

thickness. In conjunction with Camblong [63–65] they used the same model in a real-space approach (negating the need for a local approximation for the conductivity). Their model provided reasonable agreement in both CIP and CPP with semi-classical models—if quantum interference and quantum size effects are ignored. Similar results were obtained by Vedyayev *et al* [66, 67] who considered bulk spin-dependent scattering in spin-valves. Zhang and Butler [68] calculated the position-dependent conductivity without vertex corrections and then, using a phenomenological imaginary part of the self-energy, compared results from different models concluding that if there are no potential discontinuities at the interfaces then quantum effects are averaged out and the semi-classical models work well.

Attempts were made to consider the intrinsic spin-dependent electronic potential of the multilayer by Zhang and Levy [69] using the Kronig–Penney model in momentum space and by Bulka and Barnaś [70] in real space, but the full spin-polarized band structure calculation is really needed to be quantitative. The next level of complexity is to use single band models: of these, the tight-binding models are

probably the most useful as they are well suited to numerical calculations and can also be generalized to a multi band model. These models include the Stoner exchange splitting of the spin band, which introduces disorder by randomizing on-site energies and impurities by adding different atoms to the host. Examples of these models are by Asano [71] and Itoh [72] who used a spin-dependent multilayer potential and of Todorov [73] who used spin-dependent band-widths. They were successful in revealing the microscopic origin of the spin-dependent scattering, but suffered from the lack of an accurate description of the spin-polarized band structure. Itoh improved the model by calculating the self-consistent electronic structure and magnetic moments at interfaces, enabling a study of the material dependence of GMR and thermopower [74].

Even from the simple picture of GMR presented at the beginning of this review, it is clear that the d bands play a crucial role in the GMR. This role is considerably enhanced by the hybridization between the sp and d electrons. Only a multiband model is able to incorporate this information accurately into a theory. Recent decades have seen a significant advance in the calculation of realistic band structures able

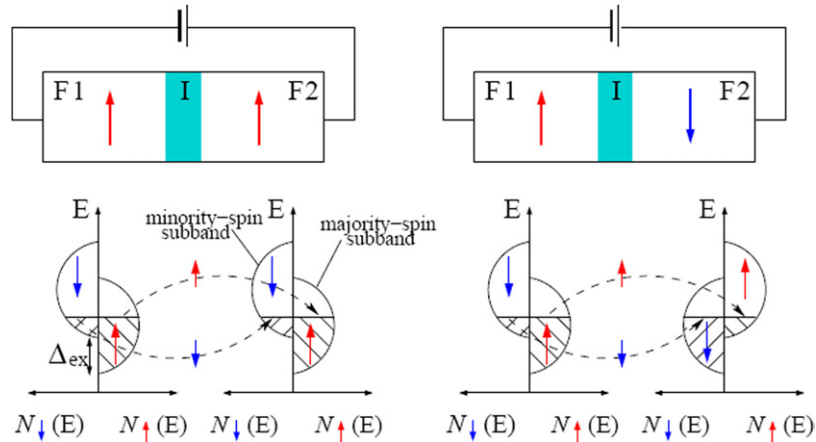


Figure 13. Schematic diagram of TMR showing the availability of empty states of the same spin orientation when the two ferromagnetic layers are aligned parallel and the lack of available states when they are aligned antiparallel. (Reprinted with permission from [147]. Copyright 2004, American Physical Society.)

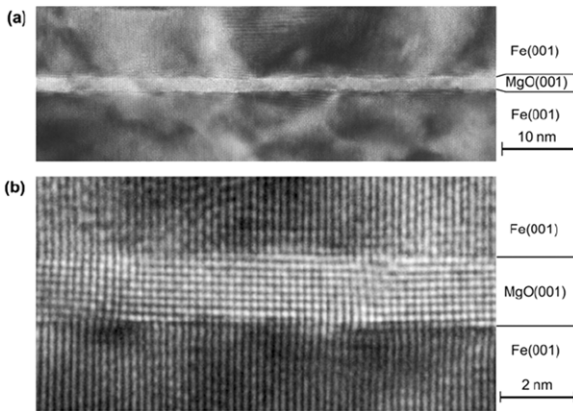


Figure 14. Cross-sectional transmission electron microscope images of an epitaxial Fe(001)/MgO(001)(1.8 nm)/Fe(001) magnetic tunnel junction. The higher resolution image in (b) is a portion of the sample imaged in (a). The vertical direction corresponds to the MgO[001](Fe[001]) axis, and the horizontal direction to the MgO[100](Fe[110]) axis. (Reprinted with permission from [90]. Copyright 2004, Nature Publishing Group.)

to reflect this reality. Most notable are the advances in *ab initio* electronic band structure calculations such as density functional theory, although multiband tight-binding models are still very effective. The difficulties in the modelling come not from the accurate description of the band structure, but in how to include the disorder. Most real structures behave diffusively and the GMR depends critically on the details of this disorder. There are a number of models which can incorporate specific types and locations of defects into the idealized structure: however, the detailed defect structure is often unknown in practice and the incorporation of the specific details therefore becomes unjustified. Realizing this, Tsymbal and Pettifor [75–77] used a simpler approach, which nonetheless introduced disorder into a realistic tight-binding band structure. They considered scattering from spin-independent scattering potentials allowing the spin dependence in the scattering to arise from the spin asymmetry of the density of states. They were able to predict values very close to experiments and demonstrated how sensitive the GMR is to

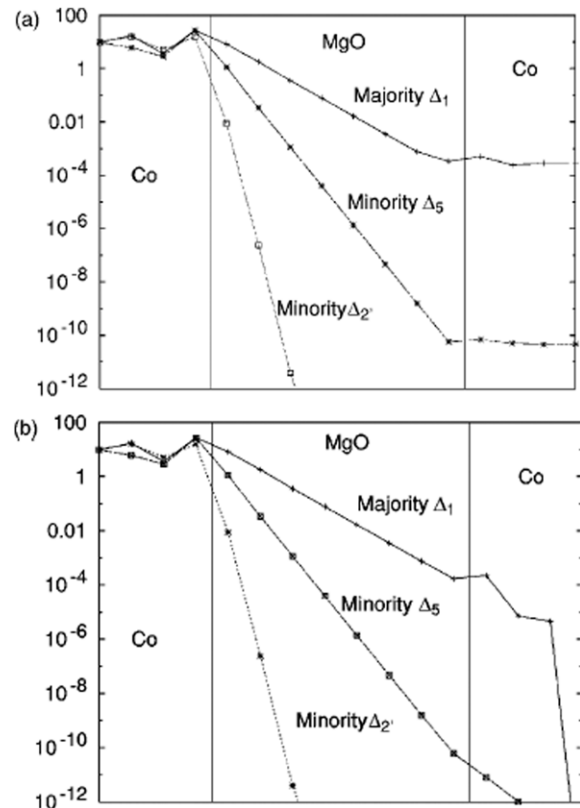


Figure 15. Model simulations from Butler [93] showing the tunnelling density of states for a Co/MgO/Co magnetic tunnel junction. The graphs show the tunnelling density of states at each atomic layer at $k_{||} = 0$ for parallel alignment at the top and antiparallel alignment at the bottom. The tunnelling is shown to be dominated by the parallel majority spin-conductance channel Δ_1 . (Reprinted with permission from figure 2 of [93]. Copyright 2004, American Physical Society.)

the disorder in the system. Figure 12 shows the density of states, conductivity and both CIP and CPP GMR as a function of electron energy for both Co/Cu and Fe/Cr multilayers.

There are a number of features still not included in these models such as magnetic disorder at the interface and the

relativistic effects needed to describe the spin-orbit scattering important in the description of the spin-diffusion length. It is also true to say, with the difficulties in accurately describing the full structure, that most researchers still turn to the semi-classical models to interpret their results.

5. Related mechanisms

The discovery of GMR has stimulated research on the spin dependence of other transport phenomena—some intimately connected to GMR such as tunnelling magnetoresistance (TMR) and others with a completely different mechanism such as colossal magnetoresistance (CMR).

5.1. Tunnelling magnetoresistance

If the two ferromagnetic electrodes are separated by a thin insulating layer, then classical electron transport through the insulator cannot take place; however, if the insulating layer is thin enough, typically a few atomic layers, then electrons are able to tunnel through the insulating barrier into available electron states on the other side. The tunnelling process is therefore dependent on the available electron states in the ferromagnetic electrodes, and, as has recently been shown, on the available channels in the insulator. We are now concerned with spin-selective band matching rather than spin-dependent scattering; however the magnetic dependence of the process is similar to a GMR structure in that the electrical resistance of the device is usually high when the magnetic orientation of the ferromagnetic layers is antiparallel and low when they are aligned. A simple picture of spin-dependent tunnelling is shown in figure 13.

The first work on TMR was in fact done as early as in 1972 on granular Ni-SiO₂ films [78] and then in the more familiar thin film sandwich structure in 1975 by Jullière [79] and by Maekawa and Gafvert in 1982 [80]. Although reporting significant results, e.g. 14% TMR in Fe/amorphous Ge/Co [79], the experiments were carried out at a low temperature and their significance was not widely recognized until interest in magnetoresistance was stimulated by the discovery of GMR. In addition, the controlled growth of thin insulating tunnel barriers was a considerable technological challenge, and one that was initially not seen as having anything other than an academic interest. This changed in 1995 when Moodera *et al* [81, 82] published room temperature TMR results: 12% in CoFe/Al₂O₃/Co, and Miyasaki *et al* [83] 18% TMR in Fe/Al₂O₃/Fe. These first generation TMR devices rely on amorphous insulating tunnel barriers and with improved growth techniques were developed to routinely deliver high TMR values of typically 50% in patterned devices.

As early as in 1999, first principles theories revealed the importance of the detailed electronic and hence crystal structure of the insulating barrier and predicted dramatic enhancements of TMR in excess of 6000% for epitaxial Fe(100)/MgO(100)/Fe(100) structures [84–87]. Values of 1000s of per cent have not been experimentally realized as yet, but values in excess of 200% have. The reasons for lower TMR values in real samples are thought to be linked to

modifications of the electronic structure at the interface—for example, the formation of FeO in Fe/MgO structures. The first experimental observations that the structure of the tunnel barrier has a strong influence on the TMR were made in 2001 in a collaboration between Fert's group in France and three groups in Spain [88]. They observed a significant enhancement of the TMR across epitaxial MgO barriers (60%) compared with amorphous Al₂O₃ (13%). These measurements were at low temperatures, but in 2004 the community was rewarded with observations of dramatic room temperature TMR values of 200% across epitaxial MgO barriers both in Japan [89, 90] and at IBM in the USA [91]. The high degree of crystalline perfection necessary for these large enhancements is beautifully illustrated by transmission electron microscopy, reproduced in a review of TMR across crystalline MgO by Yuasa and Djayaprawira [92], figure 14.

The reasons for these very large TMR values are very clearly illustrated in the model simulations of Butler's models [93]. Figure 15 shows the tunnelling density of states and reveals that in the Co/MgO/Co system the tunnelling is dominated by the parallel majority-spin conductance, Δ_1 . The other symmetries decay far more rapidly. The TMR therefore probes the spin-polarized density of states at the Fermi level for a particular symmetry.

These enhanced TMR results are not limited to MgO or Ge, and interesting effects are predicted for a wide range of insulators and semiconductor barriers. Similarly to Fert's initial work on spin-dependent impurity scattering, it is also possible to predict material combinations for which the tunnelling will be dominated by minority electrons. For example, de Teresa *et al* [94] showed that for Co, a positive spin polarization is expected at the interface with Al₂O₃, but a negative spin polarization is created at the interface with SrTiO₃ or Ce_{1-x}La_xO₂. Importantly, methods have now been found to grow textured MgO barriers on amorphous CoFeB electrodes [95], opening the way for achieving large TMR values in commercial applications.

5.2. Colossal magnetoresistance

The discovery of GMR led to an increasing appetite for large magnetoresistance effects across the scientific community—this extended to more complex materials and the discovery of CMR hit the scientific headlines in 1994 with a thousand-fold magnetoresistance in La-Ca-Mn-O films [96]. There had, in fact, been an earlier report on a similar effect in magnetic semiconductor Nd_{0.5}Pb_{0.5}MnO₃ in 1989 [97]. The mechanism for CMR is, in fact, quite different from both TMR and GMR and is related to a magnetically induced metal-to-insulator phase transition. A recent review on magnetoresistance in the ferromagnetic manganites is given by Dörr [98].

5.3. Thermal properties

It is also possible to observe the manifestations of GMR in other material properties such as thermal conductivity via the Wiedemann Franz law [99]. Further, when the interaction of electromagnetic radiation with the material is explored,

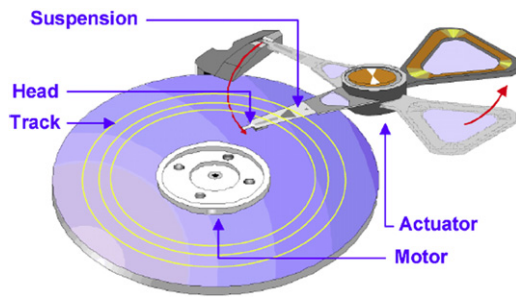


Figure 16. Schematic diagram of a hard disk platter showing recorded tracks, actuator and suspension onto which the head is attached. (Reprinted with permission from figure 3 of [106]. Copyright 2005, Elsevier.)

it is found that at long wavelengths where only intraband excitations are possible, there is a simple relationship between the complex dielectric function and the optical conductivity [100–102]. This leads to a dependence of the refractive index on the electrical conductivity enabling a series of non-contact probes of magnetoresistance to be developed in the far infrared region of the spectrum [103–105].

6. Applications

The discovery of GMR was not driven by a technological need—but its rapid development was. Unlike many scientific discoveries for which future applications are predicted or sought, GMR landed right into a community desperate for a sensitive, nanoscale magnetoresistive sensor. This drove both theoretical and practical evolution of GMR in an international explosion of both academic and industrial research, with the result that the first commercial GMR read heads appeared in hard disk drives as early as in 1997. Now that GMR magnetic sensors are a mature technology, they are finding wider application and seeking also to make a further impact on the previous semiconductor domain of random access memory (RAM).

6.1. GMR and data storage

The technology of the read head in a hard disk has evolved considerably since the invention of the hard disk in 1956. A true nanoscale device, a modern read head will typically have more than a dozen nanoscale layers, controlled on the atomic scale, subject to more than 250 processing steps and in operation ‘flies’ typically 10–15 nm above the hard disk platter which is spinning at up to 15 000 rpm. A recent review on read head sensor technology is given by Childress [106]. A schematic diagram of the overview of the hard disk showing the disk platter, actuator and location of the read–write head over the spinning platter is shown in figure 16 and the structure of the complete read–write head in figure 17.

The technology drive is for greater areal storage density, measured in Gb in^{-2} . This has risen from 0.132 Gb in^{-2} in 1991 to better than 500 Gb in^{-2} today, illustrated in the areal density growth curve from Hitachi GST in figure 18. For an 80 Gb in^{-2} longitudinal bit hard drive, the lateral bit dimensions are $200 \text{ nm} \times 30 \text{ nm}$, demanding a recording

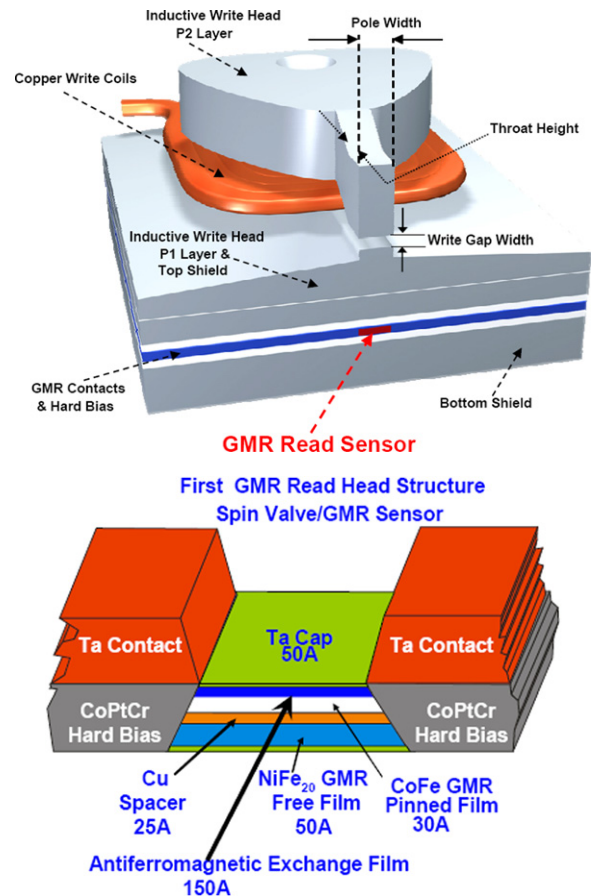


Figure 17. Schematic diagram of a read–write head showing the relative orientations of the inductive writer and the GMR read element. The bottom figure shows the detail of a spin-valve head construction including the contacts and the hard-bias. (Source: Hitachi GST.)

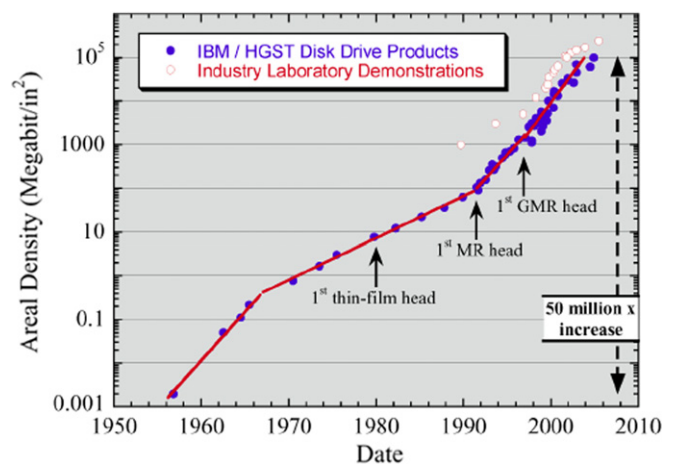


Figure 18. The annual and projected growth in areal density in IBM/Hitachi GST hard disk drives showing the increase in growth rate as different head technologies were introduced. (Reprinted with permission from figure 8 of [106]. Copyright 2005, Elsevier.)

head of similar dimensions. At the time that GMR was discovered, both the read and write components of the recording head used inductive technology. The inductive reading mechanism was the limiting factor to the increase in data density; compromised by lower magnetization, smaller

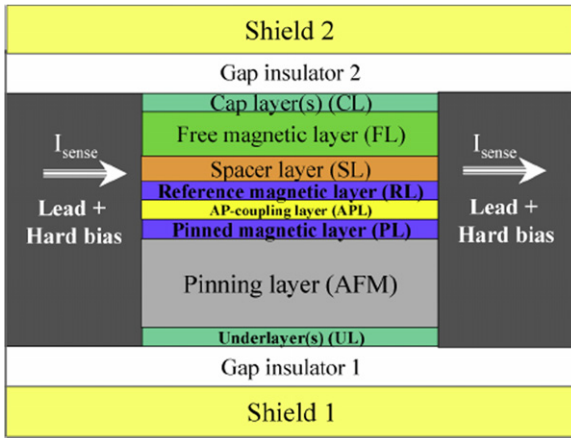


Figure 19. Schematic diagram of a typical CIP GMR sensor in the read head as viewed from the disk and showing the current flow direction. (Reprinted with permission from figure 10 of [106]. Copyright 2005, Elsevier.)

dimensions and the faster data rate presented by the decreasing bit size. The first magnetoresistive heads were introduced in the early 1990s using AMR materials which, although offering magnetoresistance values of only 1–2%, increased the rate of increase of storage density and paved the way for the introduction of GMR heads.

Antiferromagnetically coupled GMR multilayers promised significantly higher signals compared with AMR materials, but the development of the spin-valve was required to increase the field sensitivity and generate a linear response. In the original CIP spin-valve, the pinned layer was exchange biased to an antiferromagnet. This structure evolved into a more robust synthetic spin-valve in which the pinned ferromagnetic layer is in turn antiferromagnetically coupled to a reference magnetic layer, decoupled as before from the free magnetic layer by a non-magnetic spacer layer. The complete CIP structure is shown in figure 19.

The linear response is achieved by magnetically biasing the structure and ensuring that the combination of bias, anisotropy, current induced and demagnetizing fields act so that the free layer lies along the track direction, perpendicular to the reference and pinned layers which lie along the signal field. The free layer is then rotated by approximately 30° during the read-back process as illustrated in figure 20. These practical devices deliver up to 20% GMR.

As the bit size continues to decrease, CIP-GMR heads have themselves come up against limitations, primarily due to the degradation in performance that results due to edge effects, increased shunting of the electrical current and the effects on the sensor resistance due to the reduced sensor length. Many of these problems can be overcome in the CPP geometry where the current path is no longer along the sensor length and the geometry can be simplified by using the shields as electrical contacts. The structure of a CPP head is shown in figure 21.

Both CPP-GMR and TMR–GMR effects can be employed in CPP heads, each with their own advantages and disadvantages. These are concerned with mainly the resistance area (RA) product, noise considerations and signal voltage. TMR heads have a considerable advantage in the signal

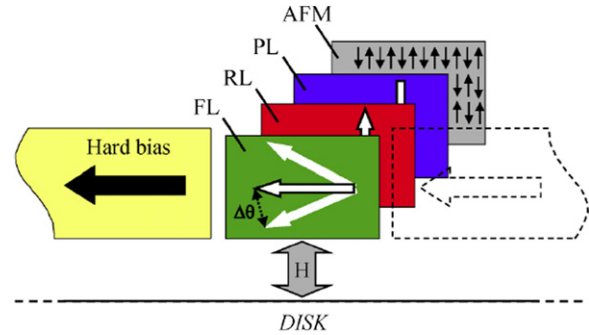


Figure 20. Schematic diagram showing the relative magnetization orientations in a typical GMR head. Shown are the hard bias, free ferromagnetic layer (FL), ferromagnetic reference layer (RL), pinned ferromagnetic layer (PL) and pinning antiferromagnetic layer (AFM). H represents the vertical magnetic field direction of the magnetic transitions on the disk which act to rotate the horizontally orientated FL by an angle $\Delta\theta$ as shown. (Reprinted with permission from figure 11 of [106]. Copyright 2005, Elsevier.)

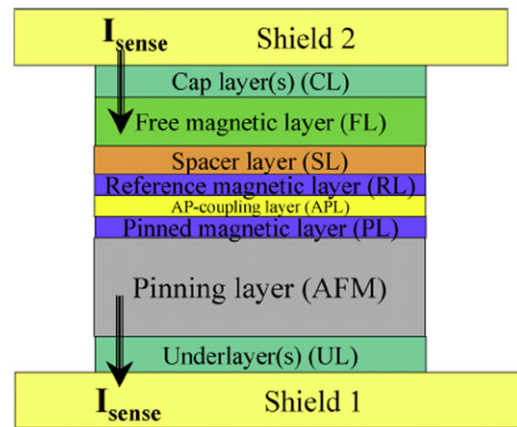


Figure 21. Schematic diagram of a typical CPP GMR sensor in the read head as viewed from the disk and showing the current flow direction. (Reprinted with permission from figure 15 of [106]. Copyright 2005, Elsevier.)

voltage in that the TMR effect is usually greater than 20%. However, the intrinsically higher resistance of a TMR structure can cause noise problems and a high RC time constant reducing the operating bandwidth. Addressing the high RA product involves reducing the barrier height and the tunnelling barrier thickness: however the problem of shot noise, inherent to the tunnelling process, still remains. The processing challenges associated with commercializing a TMR head are quite considerable, although there is a slight advantage that the TMR effect itself is extremely localized at the junction. The case for CPP-TMR heads has been significantly enhanced by the discovery of exceptionally high TMR effects across crystalline MgO barriers and TMR effects as high as 150% have been achieved in devices with RA products as low as $2 \Omega \mu m^2$ [107]. CPP-GMR heads have an inherently lower RA product reducing noise and increasing the bandwidth. However, the GMR effect is similar to that of CIP, so that to achieve a usable signal voltage, high current densities must be used. The thermal effects of the high current densities are ameliorated by the substantial heat sink provided by the shields, but there remains the problem of the spin-transfer

torque introduced by the spin-polarized current (see section 7) introducing an additional magnetic instability. It is possible to overcome this by using a dual spin-valve structure, at the expense of increasing the sensor stack size. Recently, there has been some success in increasing the GMR effect in all-metal structures by using ferromagnetic Heusler alloys [108]. Further improvement might be achieved by using a nano-oxide layer to confine the current [109]. Future directions in magnetic data storage technology, such as the move to perpendicular recording media, thermally assisted recording and patterned media, will still require a similar recording head head designs succeeding below dimensions of 30 nm.

6.2. GMR sensors

The successful commercialization of GMR sensors in hard disk read heads has opened the way to the application of GMR sensors in other situations where size, speed and sensitivity are important parameters [110]. Examples can be found in a wide variety of situations such as nanoscale arrays of GMR sensors for 100 μm scale spatially resolved eddy current detection [111], biological sensors for molecule tagging [112, 113], galvanic isolators [114], traffic control, engine management systems, magnetic separation and electronic compasses.

6.3. Magnetic random access memory

In addition to the phenomenal contribution that GMR has made to magnetic hard disk storage devices, there has been considerable effort, especially by Motorola/Freescale, IBM [115] and Infineon, for developing a magnetic random access memory (MRAM) to compete with DRAM and SRAM which would have the advantages of non-volatility, radiation hardness and low energy consumption. In an MRAM device, magnetic tunnel junctions (MTJs) are both the storage and the read element. A typical MRAM architecture is shown in figure 22 [116] where the digital '1' and '0' states are achieved by an MTJ in either the parallel anti-aligned or the aligned state.

MTJs took over from GMR devices in MRAM applications due to their high magnetoresistance, high resistance, which makes them compatible with CMOS technology, ease of scaling to small dimensions and a weak variation with temperature. Developments in spin-transfer switching and the enhanced MR values found with crystalline and textured barriers have recently given new impetus to these developments.

7. Spin transfer and current induced switching

In 1996 theoreticians Berger [117] and Slonczewski [118] realized that a spin-polarized current was capable of inducing a spin-transfer torque which could be engineered to switch the magnetic orientation of a ferromagnetic layer—providing a method of switching a magnetic layer without the application of a magnetic field. The first experiments were conducted on magnetic pillars in 2000 by Katine *et al* [119] and a schematic diagram of their experiment and their results are shown in figure 23.

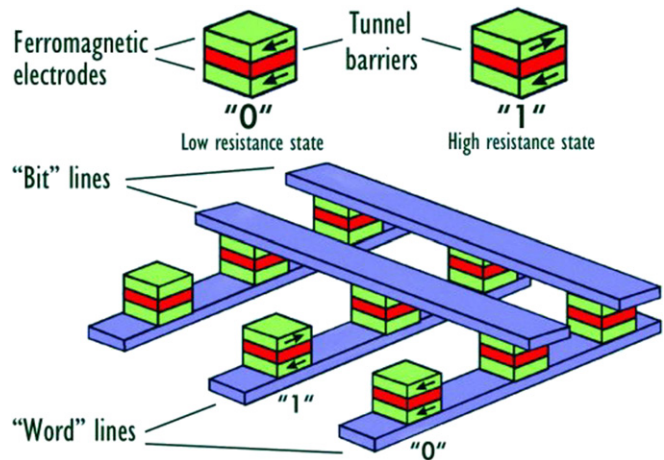


Figure 22. Schematic diagram of a possible MRAM architecture. The memory cells are shown at the top to be magnetic tunnel junctions with the two memory states represented by parallel and antiparallel alignment of the ferromagnetic layers. The bits are assembled and connected in an array as shown below creating 'word lines' and 'bit lines'. The voltage across a single bit can be read by connecting to the array appropriately and the magnetization orientation of the bits changed by the magnetic field created from the passing of a write current. (Reprinted with permission from figure 1 of [116]. Copyright 2003, European Physical Society.)

The nanopillars in these experiments contained two Co layers of different thickness separated by a non-magnetic Cu layer. Consider the situation where the two layers are initially antiparallel and the current travels from the thick to the thin layer. The current is spin polarized by the first Co layer and as it enters the second Co layer, its spin rotates due to the exchange interaction to become aligned with the local magnetization. However, due to conservation of spin, there is now a spin torque acting on the magnetization of the ferromagnet, which if the current density is high enough can be sufficient to switch the layer. The reverse is true when the ferromagnetic layers are parallel, then the spin-polarized current flowing from the thin layer to the thick layer will switch the thin layer into antiparallel alignment. The most direct way to detect magnetization switches is by the GMR that results from the change in the relative magnetic orientation of the two layers. These resistance changes are also shown in figure 23.

Current induced switching provides a very attractive method for switching the GMR or TMR in a spintronic device without applying a magnetic field. This is particularly attractive for MRAM where the stray fields from the write current have the potential to switch neighbouring elements. It is also important to realize the potential of a high current density spin-polarized current to destabilize the magnetization of a ferromagnetic element. This is now a recognized instability problem in the sense layer of a CPP spin-valve. The technological challenge to achieving current induced switching is to provide sufficient current density, typically 10^7 A cm^{-2} , the solution usually being to pattern magnetic nanopillars. An alternative is to use a weaker ferromagnetic material such as Mn doped GaMnAs as demonstrated by Elsen *et al*, where switching was achieved at a much lower current density of 10^5 A cm^{-2} [120].

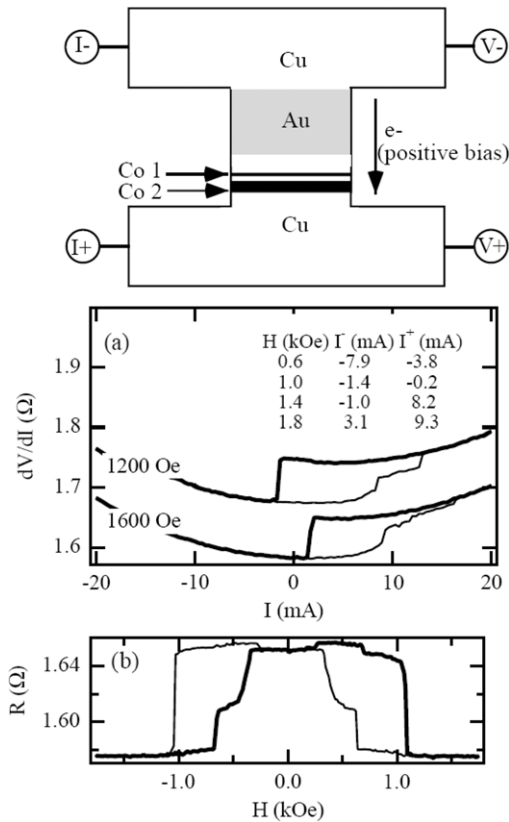


Figure 23. (Top) The nanopillar structure and (bottom) the data from the first experimental report of spin-transfer torque by Katine *et al* [119]. The ~130 nm wide nanopillars were constructed by electron beam lithography, evaporation, lift-off and ion milling after first sputter depositing the multilayer structure: Si/Cu(120 nm)/Co(10 nm)/Cu(6 nm)/Co(2.5 nm)/Cu(15 nm)/Pt(3 nm)/Au(60 nm). As indicated in the diagram, positive bias is defined as the electron flow from the thin to the thick layer. In the dV/dI curves, the light line shows the increasing current sweep and the dark line the decreasing current sweep. With the magnetic field applied, the Co layers are originally in the parallel aligned low resistance state when $I = 0$. When the current reaches a threshold value (I^+) the magnetization direction of the thin Co layer switches and the resistance increases. There are two jumps in resistance shown at approximately 9 and 13 mA for the $H = 1200$ Oe case. During the negative current sweep, the threshold current for the switch back to parallel alignment (I^-) occurs at negative bias, giving hysteretic behaviour. The magnetization direction of the thick layer remains fixed throughout. Two sets of results are shown at different applied fields which have been offset for clarity. The inset table gives the critical current values at which the device deviates from the parallel configuration (I^+) to the antiparallel configuration (I^-) showing the higher current densities required for switching in higher applied magnetic fields. The bottom graph shows the magnetoresistance of the structure in zero bias. (Reprinted with permission from figures 1 and 2 [119]. Copyright 2000, American Physical Society.)

An interesting application of spin-transfer torque is in microwave generation where the spin torque induces magnetic precessions rather than irreversible switching [121]. This possibility arises from the interplay of the spin-transfer torque acting on the magnetic element as calculated by spin-transport equations and magnetization excitations generated by this spin-torque described by non-linear dynamics. In simple spin torque systems, the precession regime is accessed above a

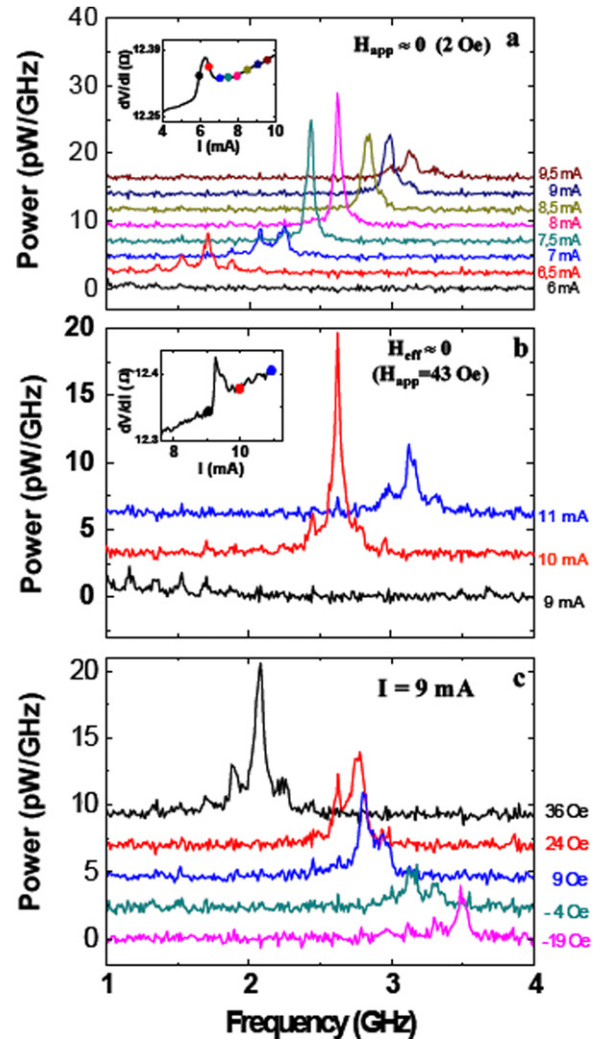


Figure 24. The results of Boulle *et al* [122] for the microwave power spectra of Co(8 nm)/Cu(10 nm)/NiFe(8 nm) nanopillars with ‘wavy’ angular dependence of the spin-transfer torque. Graphs (a) and (b) show the spectra for different currents in small applied magnetic fields with the insets showing dV/dI . In (a) the applied field is 2 Oe and in (b) the field applied of 43 Oe is calculated to give zero effective magnetic field taking into consideration the contribution from the dipolar field. Graph (c) shows the spectra for a current of 9 mA at different applied fields. (Reprinted with permission from figure 3 of [122]. Copyright 2007, Nature Publishing Group.)

threshold magnetic field. However, in a recent work by Boulle *et al* voltage oscillations at microwave frequencies have been obtained without the application of a magnetic field [122]. Large angle magnetic precessions are achieved by designing structures with different spin-diffusion lengths (e.g. Co and NiFe) for the two ferromagnetic materials, resulting in a ‘wavy’ angular dependence of the torque. Figure 24 shows the characteristic precession peaks at different microwave frequencies for different current densities in zero applied field.

The next step in this research is to work on increasing the output power which is being addressed by synchronizing a number of these spin-torque oscillating elements electrically [123, 124].

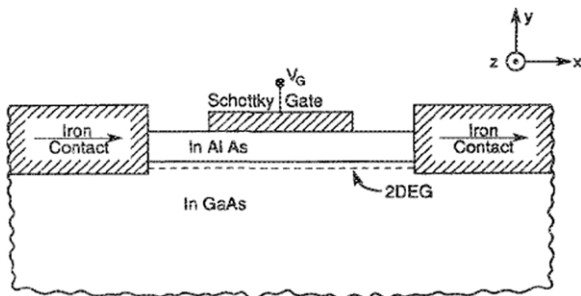


Figure 25. Schematic diagram of the proposed Datta–Das electron wave analogue of the electro-optic light modulator [125]. A spin-polarized current is injected and analysed by the Fe contacts. Spin precession in the 2DEG will occur due to the Rashba effect causing spin–orbit coupling and controlled by the gate voltage. (Reprinted with permission from figure 1 of [125]. Copyright 1990, American Institute of Physics.)

8. Semiconductor and organic spintronics

GMR has directly led to a reassessment of how we can manipulate the electron in an electric circuit. The realization that the spin of the electron can be addressed to manipulate the spin of an electron as well as its charge has created a new wide-reaching research field of spintronics. Progressing beyond the early (and now usefully employed) all-metal GMR devices it is possible to envisage active semiconductor devices where the versatility of semiconductor device technology, such as the manipulation of the current using a gate voltage and the coupling to optics, can be given an extra degree of freedom by the electron spin. The first idea for a hybrid ferromagnetic metal/semiconductor device is credited to Datta and Das in 1990 [125]; however, practical realization has proved a scientific and technological challenge. Their spin-field effect transistor (spin FET) in which spin-polarized electrons are injected into a 2-DEG channel has become an iconic spintronic device and is shown in figure 25. Early successful devices progressively increased the functionality of the relatively simple all-metal GMR devices. The first 3-terminal device was created by Johnson [126] who made a third contact to the central layer of a GMR material creating an all-metal spin transistor—albeit with no gain. The spin-valve transistor shown in figure 26 [127, 128] was the first device to combine ferromagnetic and semiconductor materials and operated by sandwiching a spin-valve between two semiconductors creating different barrier height Schottky barriers at the interfaces. Transmission across the second Schottky barrier is controlled by the energy loss of the electrons as they traverse the spin-valve which in turn is controlled by the applied magnetic field. This transistor does provide a magnetically controlled current gain (although it is less than unity) and has potential as a magnetic field sensor. Gregg *et al* [129, 130] have designed and produced a Si based spin transistor which although not optimized does yield a current gain greater than unity and operates at useable currents. An optical device has been successfully created by Mostnyi *et al* [131] in which Fe is used to inject spin-polarized current into an LED across a tunnel junction, generating circularly polarized light.

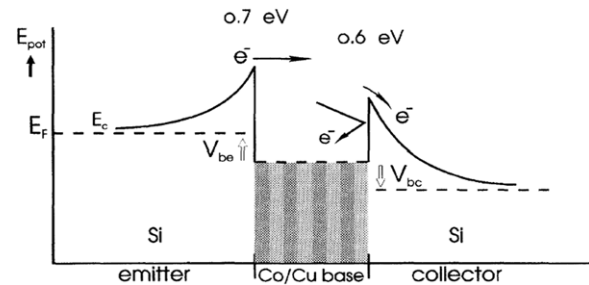


Figure 26. Schematic energy band diagram of the Monsma spin-valve transistor under forward bias [127]. Hot electrons are injected across the emitter Schottky barrier and lose energy as they traverse the GMR Co/Cu multilayer base of the transistor. The energy of the electrons as they arrive at the (lower) collector Schottky barrier is controlled by the scattering in the base and the collector current is consequently dependent on the magnetic orientation of the GMR base multilayer. (Reprinted with permission from figure 2 of [127]. Copyright 1995, American Physical Society.)

The challenges in developing hybrid spintronics devices are both scientific and technological. The biggest challenge is that of spin injection from a ferromagnetic material into a semiconductor—in such a way as to maintain a useful spin accumulation in the semiconductor, and the inverse problem of extracting the spin at the detection end of the device. The difficulties arise principally because most ferromagnetic material are metals with a considerably lower electrical resistance than a semiconductor. There are various materials solutions to this problem: develop a room temperature magnetic semiconductor thereby removing the material mismatch [132–134]; use a ferromagnetic oxide material such as Fe_3O_4 as the ferromagnetic material, thereby reducing the impedance mismatch [135, 136] or insert a Schottky or tunnel barrier at the interface between the ferromagnet and the semiconductor [137–139]. All these approaches have their merits and are being actively pursued. There are also considerations that must be made towards the geometry of the device. For example, if a tunnel junction is used to inject spins into a spin FET then the dwell time of the electrons becomes significant [140]. For the device to work effectively the spin lifetime must be much longer than the dwell time. This is difficult to achieve in lateral geometry and is one of the reasons why measured effects have not exceeded 1%. Vertical geometry is clearly preferable, but has its own technological problems, not least those of the quality of the semiconductor and its interface with the ferromagnet. In fact, the spin lifetimes in semiconductors, although still a constraining factor in the device design, are helpfully considerably longer than in metals. A beautiful series of optical experiments by Awschalom *et al* [141, 142] have very clearly revealed the longevity and robustness of the spin coherence in semiconductors.

Recently, the advantages of organic materials in spintronic materials have been recognized (reviewed in 2007 by Naber *et al* [143]). For example, carbon nanotubes and graphene have very long spin lifetimes (of order 50 ns) and high velocity. In 2007 Mathur *et al* reported a simple organic spintronic device in which two ferromagnetic manganite pads were connected by

a multi-walled carbon nanotube and magnetoresistive effects of 61% at $T = 5$ K observed [144]. Comprehensive reviews and summaries of spintronics can be found in Awschalom [145], Gregg [30], Jonker and Flatte [140], Wolf [114], Xu [146] and Zutic [147].

Working with electrons offers the potential for scaling down to single electron devices and spin-dependent Coulomb blockade. The construction and measurement of such devices is a considerable challenge, but work on single electron transistors is an area of continuing interest and challenge [148–150]. Electron spins have also found a niche in the challenging search for a quantum bit in the design of a quantum computer. In one proposal, the spin confined in a quantum dot has been proposed as a candidate [151] and in another the quantum bit is a phosphorous nucleus embedded in Si which communicates via the hyperfine interaction with localized electron spins and by the exchange interaction with neighbouring spins [152].

9. Concluding remarks

The discovery of GMR and the accompanying antiferromagnetic coupling provided the stimulus for a new outlook on electron transport and the magnetic properties of materials. An understanding of the mechanisms responsible and the practical ability to prepare and characterize nanoscale materials stimulated creativity and the realization of designer magnetic materials. The pace of development was unquestionably driven by the rigorous demands of the magnetic data storage industry which made the GMR sensor a practical entity and a true nanoscale device. The journey into this new field of spintronics has been rich and rewarding and continues to provide new ideas, possibilities and increasingly widespread applications. Along the way we have seen quantum mechanical magnetic tunnel junctions manufactured on a commercial scale, used the spin of the electron to reverse a magnetic moment and witnessed an enormous international effort to find new magnetic materials such as magnetic semiconductors tailored for our needs. All of our creative expertise will be needed to continue this journey into the versatile world of hybrid metal/semiconductor or magnetic semiconductor spintronics which will test our ability to design magnetic materials and create ever more interesting ways to exploit the spin of the electron.

Acknowledgment

Bruce Gurney and Hitachi GST are gratefully acknowledged for their permission to use the diagram in figure 17. The author has appreciated the advice and helpful comments of Jeff Childress at Hitachi GST and Stuart Parkin at IBM. The author is also grateful to all the authors who willingly gave their permission for their figures to be reproduced in this article.

References

- [1] Thomson W 1857 *Proc. R. Soc.* **8** 546
- [2] Binasch G, Grünberg P, Saurenbach F and Zinn W 1989 *Phys. Rev. B* **39** 4828
- [3] Baibich M N, Broto J M, Fert A, Nguyen van Dau F, Petroff F, Eitenne P, Creuzet A, Friederich A and Chazeles J 1988 *Phys. Rev. Lett.* **61** 2472
- [4] See for example Cullity B D 1972 *Introduction to Magnetic Materials (Addison-Wesley Series in Metallurgy and Materials)* (Reading, MA: Addison-Wesley)
- Jiles D 1998 *Introduction to Magnetism and Magnetic Materials* (Boca Raton, FL: CRC Press)
- [5] Campbell I A and Fert A 1982 Transport properties of ferromagnets *Ferromagnetic Materials* ed E P Wohlfarth (Amsterdam: North Holland) vol 3 p 747
- [6] Englert E 1932 *Ann. Phys., Lpz.* **14** 589
- [7] Gerlach W 1932 *Ann. Phys., Lpz.* **12** 849
- [8] Potter H H 1931 *Proc. R. Soc. A* **132** 559
- [9] Mott N F 1936 *Proc. R. Soc. A* **153** 699
- [10] Fert A and Campbell I A 1968 *Phys. Rev. Lett.* **21** 1190
- [11] Fert A and Campbell I A 1976 *J. Phys. F: Metal Phys.* **6** 849
- [12] Grünberg P, Schreiber R, Pang Y, Brodsky M B and Sowers H 1986 *Phys. Rev. Lett.* **57** 2442
- [13] Majkrzak C F, Cable J W, Kwo J, Hong M, McWhan D B, Yafet Y and Waszczak J V 1986 *Phys. Rev. Lett.* **56** 2700
- [14] Salamon M B, Sinha S, Cunningham J E, Erwin R E, Borchers J and Flynn C P 1986 *Phys. Rev. Lett.* **56** 259
- [15] Ruderman M A and Kittel C 1954 *Phys. Rev.* **96** 99
- [16] Ortega J E, Himpfel F J, Mankey G J and Willis R F 1993 *Phys. Rev. B* **47** 1540
- [17] Parkin S S P 1991 *Phys. Rev. Lett.* **67** 3598
- [18] Heinrich B, Celinski Z, Cochran J F, Muir W B, Rudd J, Zhong Q M, Arrott A S, Myrtle K and Kirschner J 1990 *Phys. Rev. Lett.* **64** 673
- [19] Cochran J F, Rudd J, Muir W B, Heinrich B and Celinski Z 1990 *Phys. Rev. B* **42** 508
- [20] Weber W, Allenspach R and Bischof A 1995 *Europhys. Lett.* **31** 491
- [21] Parkin S S P, More N and Roche K P 1990 *Phys. Rev. Lett.* **64** 2304
- [22] Grünberg P 1989 *DE Patent* 3820475
Grünberg P 1989 *US Patent* 4949039
- [23] Fert A and Campbell I A 1971 *J. Physique* **32** (suppl. C1) 46
- [24] Marrows C H 2005 *Adv. Phys.* **54** 585
- [25] Viret M, Vignoles D, Cole D, Coey J M D, Allen W, Daniel D S and Gregg J F 1996 *Phys. Rev. B* **53** 8464
- [26] Levy P M and Zhang S 1997 *Phys. Rev. Lett.* **79** 5110
- [27] Gregg J F, Allen W, Ounadjela K, Viret M, Hehn M, Thompson S M and Coey J M D 1996 *Phys. Rev. Lett.* **77** 1580
- [28] Garcia N, Munoz M and Zhao Y W 1999 *Phys. Rev. Lett.* **82** 2923
- [29] Bruno P 1999 *Phys. Rev. Lett.* **83** 2425
- [30] Gregg J F, Petj I, Jouguelet E and Dennis C 2002 *J. Phys. D: Appl. Phys.* **35** R121
- [31] Dieny B, Speriosu V S, Gurney B A, Parkin S S P, Wilhoit D R, Roche K P, Metin S, Peterson D T and Nadimi S 1991 *J. Magn. Magn. Mater.* **93** 101
- [32] Pratt W P Jr, Loloee R, Schroeder P A and Bass J 1991 *Phys. Rev. Lett.* **66** 3060
- [33] Dieny B, Speriosu V, Parkin S S P, Gurney B, Wilhoit D R and Mauri D 1991 *Phys. Rev. B* **43** 1297
- [34] Dieny B 1994 *J. Magn. Magn. Mater.* **136** 335
- [35] Dieny B, Speriosu V S, Metin S, Parkin S S P, Gurney B A, Baumgart P and Wilhoit D R 1991 *J. Appl. Phys.* **69** 4774
- [36] Chaiken A, Lubitz P, Krebs J J, Prinz G A and Harford M Z 1991 *Appl. Phys. Lett.* **59** 240
- [37] Parkin S S P 1993 *Phys. Rev. Lett.* **71** 1641
- [38] Parkin S S P, Bhadra R and Roche K P 1991 *Phys. Rev. Lett.* **66** 2152

- [39] Parkin S S P, Li Z G and Smith D J 1991 *Appl. Phys. Lett.* **58** 2710
- [40] Nicholson D M C, Butler W H, Zhang X-G, MacLaren J M, Gurney B A and Speriosu V S 1994 *J. Appl. Phys.* **76** 6905
- [41] Coehoorn R 1993 *J. Magn. Magn. Mater.* **121** 432
- [42] Itoh H, Inoue J, Maekawa S 1993 *Phys. Rev. B* **47** 5809
- [43] de Groot R A, Mueller F M, van Engen P G and Buschow K J H 1983 *Phys. Rev. Lett.* **50** 2024
- [44] Hwang Y and Cheong S-W 1997 *Science* **278** 1607
- [45] Dieny B, Humbert P, Speriosu V S and Gurney B A 1992 *Phys. Rev. B* **45** 806
- [46] Berkowitz A E, Mitchell J R, Carey M J, Young A P, Zhang S, Spada F E, Parker F T, Hutten A and Thomas G 1992 *Phys. Rev. Lett.* **68** 374
- [47] Xiao J Q, Jiang J S and Chien C L 1992 *Phys. Rev. Lett.* **68** 3749
- [48] Thompson S M *et al* 1993 *Phil. Mag.* **B 68** 923
- [49] Zhang S and Levy P M 1991 *J. Appl. Phys.* **69** 4786
- [50] Zhang S, Levy P M 1993 *J. Appl. Phys.* **73** 5315
- [51] Gregg J F, Thompson S M, Dawson S J, Ounadjela K, Staddon C R, Hamman J, Fermon C, Saux G and O'Grady K 1994 *Phys. Rev. B* **49** 1064
- [52] Tsymbal E Yu and Pettifor D G 2001 *Solid State Physics* ed H Ehrenreich and F Spaepen (New York: Academic) vol 56 p 113
- [53] Camley R E, Barnaś J 1989 *Phys. Rev. Lett.* **63** 664
- [54] Barnaś J, Fuss A, Camley R E, Grünberg P and Zinn W 1990 *Phys. Rev. B* **42** 8110
- [55] Valet T and Fert A 1993 *Phys. Rev. B* **48** 7099
- [56] Johnson M and Silsbee R H 1987 *Phys. Rev. B* **35** 4959
- [57] Johnson M and Silsbee R H 1988 *Phys. Rev. Lett.* **60** 377
- [58] van Son P C, van Kempen H and Wyder P 1988 *Phys. Rev. Lett.* **58** 2271
- [59] Johnson M 1991 *Phys. Rev. Lett.* **67** 374
- [60] Lee S F, Pratt W P Jr, Yang Q, Holody P, Loloee R, Schroeder P A and Bass J 1993 *J. Magn. Magn. Mater.* **118** L1
- [61] Levy P M, Zhang S and Fert A 1990 *Phys. Rev. Lett.* **65** 1643
- [62] Zhang S, Levy P M and Fert A 1992 *Phys. Rev. B* **45** 8689
- [63] Camblong H E and Levy P M 1992 *Phys. Rev. Lett.* **69** 2835
- [64] Camblong H E and Levy P M 1993 *J. Appl. Phys.* **73** 5533
- [65] Camblong H E 1995 *Phys. Rev. B* **51** 1855
- [66] Vedyayev A, Dieny B and Ryzhanova N 1992 *Europhys. Lett.* **19** 329
- [67] Dieny B, Vedyayev A and Ryzhanova N 1993 *J. Magn. Magn. Mater.* **121** 366
- [68] Zhang X G and Butler W H 1995 *Phys. Rev. B* **51** 10085
- [69] Zhang S and Levy P M 1993 *Magnetic Ultrathin Films, Multilayers and Surfaces, Interfaces and Characterisation, MRS Materials Research Society Symp. Proc.* (Pittsburgh, PA: MRS Society) **313** 53
- [70] Bulka B R and Barnaś J 1995 *Phys. Rev. B* **51** 6348
- [71] Asano Y, Oguri A and Maekawa A 1993 *Phys. Rev. B* **48** 6192
- [72] Itoh H, Inoue J and Maekawa S 1995 *Phys. Rev. B* **51** 342
- [73] Todorov T N, Tsymbal E Yu and Pettifor D G 1996 *Phys. Rev. B* **54** R12685
- [74] Itoh H, Inoue J and Maekawa S 1993 *Phys. Rev. B* **47** 5809
- [75] Tsymbal E Yu and Pettifor D G 1996 *J. Phys.: Condens. Matter* **8** L569
- [76] Tsymbal E Yu and Pettifor D G 1996 *Phys. Rev. B* **54** 15314
- [77] Tsymbal E Yu and Pettifor D G 1997 *J. Appl. Phys.* **81** 4579
- [78] Gittleman J I, Goldstein Y and Bozowski S 1972 *Phys. Rev. B* **5** 3609
- [79] Julliere M 1975 *Phys. Lett. A* **54** 225
- [80] Maekawa S and Gäfvert U 1982 *IEEE Trans. Magn.* **18** 707
- [81] Moodera J S, Kinder L R, Wong T M and Meservey R 1995 *Phys. Rev. Lett.* **74** 3273
- [82] Moodera J and Mathon G 1999 *J. Magn. Magn. Mater.* **200** 248
- [83] Miyazaki T and Tezuka N 1995 *J. Magn. Magn. Mater.* **139** L231
- [84] MacLaren J M, Zhang X-G, Butler W H and Wang X 1999 *Phys. Rev. B* **59** 5470
- [85] Butler W H, Zhang X-G, Schulthess T C and MacLaren J M 2001 *Phys. Rev. B* **63** 054416
- [86] Zhang X-G, Butler W H and Bandyopadhyay A 2003 *Phys. Rev. B* **68** 092402
- [87] Mathon J and Umerski A 2001 *Phys. Rev. B* **63** 220403(R)
- [88] Bowen M *et al* 2001 *Appl. Phys. Lett.* **79** 1655
- [89] Yuasa S, Fukushima A, Nagahama T, Ando K and Suzuki Y 2004 *Japan. J. Appl. Phys.* **43** L588
- [90] Yuasa S, Nagahama T, Fukushima A, Suzuki Y and Ando K 2004 *Nature Mater.* **3** 868
- [91] Parkin S S P, Kaiser C, Panchula A, Rice P M, Hughes B, Samant M and Yang S-H 2004 *Nature Mater.* **3** 862
- [92] Yuasa S and Djayaprawira D D 2007 *J. Phys. D: Appl. Phys.* **40** R337
- [93] Zhang X-G and Butler W H 2004 *Phys. Rev. B* **70** 172407
- [94] De Teresa J M, Barthelemy A, Fert A, Contour J P, Montaigne F, Seneor P 1999 *Science* **286** 507
- [95] Djayaprawira D D, Tsunekawa K, Motonobu N, Maehara H, Yamagata S, Watanabe N, Yuasa S, Suzuki Y and Ando K 2005 *Appl. Phys. Lett.* **86** 092502
- [96] Jin S, Tiefel T H, McCormack M, Fastnacht R A, Ramesh R and Chen L H 1994 *Science* **264** 413
- [97] Kusters R M, Singleton J, Keen D A, McGreevy R and Hayes W 1989 *Physica B: Condens. Matter* **155** 362
- [98] Dörr K 2006 *J. Phys. D: Appl. Phys.* **39** R125
- [99] Daniel D, Gregg J F, Thompson S M, Coey J M D, Fagan A, Ounadjela K, Fermon C and Saux G 1995 *J. Magn. Magn. Mater.* **140** 493
- [100] Jacquet J C and Valet T 1995 *Materials Research Society Proceedings* (Pittsburgh: PA) vol 384 p 477
- [101] Baxter R J, Pettifor D G, Tsymbal E Y, Bozec D, Matthew J A D and Thompson S M 2003 *J. Phys. Condens. Matter* **15** L695
- [102] Mennicke R T, Bozec D, Kravets V G, Vopsaroiu M, Matthew J A D and Thompson S M 2005 *J. Magn. Magn. Mater.* **303** 92
- [103] Granovskii A, Kuýmichev M V and Clerc J P 1999 *J. Exp. Theor. Phys.* **89** 955
- [104] Vopsaroiu M, Bozec D, Marrows C H, Perez M, Matthew J A D and Thompson S M 2004 *Phys. Rev. B* **70** 214423
- [105] Stirk S M, Thompson S M, Mennicke R T, Lee A F and Matthew J A D 2006 *Appl. Phys. Lett.* **88** 022502
- [106] Childress J R and Fontana R E Jr 2005 *C. R. Physique* **6** 997
- [107] Tsunekawa K, Djayaprawira D D, Nagai M, Maehara H, Yamagata S, Watanabe N, Yuasa S, Suzuki Y and Ando K 2005 *Appl. Phys. Lett.* **87** 072503
- [108] Childress J R *et al* 2008 *IEEE Trans. Magn.* **44** 90
- [109] Oshima H, Nagasaka K, Seyama Y, Jogo A, Shimizu Y, Tanaka A and Miura Y 2003 *IEEE Trans. Magn.* **39** 2377
- [110] Daughton J, Brown J, Beech R, Pohm A and Kude W 1994 *IEEE Trans. Magn.* **30** 4608
- [111] Smith C H, Schneider R W, Dogaru T and Smith S T 2003 *Rev. Prog. Quant. Nondestr. Eval.* **23** 23 406
- [112] Baker D A, Brown J L and Smith C H 2006 *Med. Device Diagn. Indust.* **28** 112
- [113] Li G, Sun S, Wilson R J, White R L, Pourmand N and Wang S X 2006 *Sensors Actuators A* **126** 98
- [114] Wolf S A, Awschalom D D, Buhrman R A, Daughton J M, von Molnár S, Roukes M L, Chtchelkanova A Y and Treger D M 2001 *Science* **294** 1488
- [115] Gallagher W J, Parkin S S P 2006 *IBM J. Res. Dev.* **50** 5
- [116] Fert A, George J-M, Jaffrès H, Mattana R and Seneor P 2003 *Europhys. News* **34** (6) 227 (<http://www.europhysicsnews.com>)

- [117] Berger L 1996 *Phys. Rev. B* **54** 9353
- [118] Slonczewski J C 1996 *J. Magn. Magn. Mater* **159** L 1
- [119] Katine J A, Albert F J, Buhrman R A, Myers E B and Ralph D C 2000 *Phys. Rev. Lett.* **84** 3149
- [120] Elsen, M, Boulle O, George J-M, Jaffrès H, Mattana R, Cros V, Fert A, Lemaître A, Giraud R and Faini G 2006 *Phys. Rev. B* **73** 035303
- [121] Kiselev S I, Sankey J C, Krivorotov I N, Emley N C, Schoelkopf R J, Buhrman R A and Ralph D C 2003 *Nature* **425** 380
- [122] Boulle O, Cros V, Grollier J, Pereira L G, Deranlot C, Petroff F, Faini G, Barnaś J and Fert A 2007 *Nature Phys.* **3** 492
- [123] Kaka S, Pufall M R, Rippard W H, Silva T J, Russek S E and Katine J A 2005 *Nature* **437** 389
- [124] Mancoff F B, Rizzo N D, Engel B N and Tehrani S 2005 *Nature* **437** 393
- [125] Datta S and Das B 1990 *Appl. Phys. Lett.* **56** 665
- [126] Johnson M 1993 *Science* **260** 320
- [127] Monsma D J, Lodder J C, Popma J A and Dieny B 1995 *Phys. Rev. Lett.* **74** 5260
- [128] Jansen R 2003 *J. Phys. D: Appl. Phys.* **36** R289
- [129] Gregg J F *et al* 1997 *J. Magn. Magn. Mater.* **175** 1
- [130] Dennis C L, Tiusan C V, Gregg J F, Ensell G J and Thompson S M 2005 *IEE Proc. Circuits Devices Syst.* **152** 340
- [131] Motsnyi V F, Van Dorpe P, Van Roy W, Goovaerts E, Safarov V I, Borghs G and De Boeck J 2003 *Phys. Rev. B* **68** 245319
- [132] Ohno H, Shen A, Matsukura F, Oiwa A, Endo A, Katsumoto S and Iye Y 1996 *Appl. Phys. Lett.* **69** 363
- [133] Dietl T, Ohno H, Matsukura F, Cibert J and Ferrand D 2000 *Science* **287** 1019
- [134] Ohno Y, Young D K, Beschoten B, Matsukura F, Ohno H and Awschalom D D 1999 *Nature* **402** 790
- [135] Matsumoto Y, Murakami M, Shono T, Haesegawa T, Fukumura T, Kawasaki M, Ahmet P, Chikyow T, Koshishara S and Koinuma H 2001 *Science* **291** 854
- [136] Lu Y X, Claydon J S, Xu Y B, Thompson S M, Wilson K and van der Laan G 2004 *Phys. Rev. B* **70** 233304
- [137] Borges R P, Dennis C L, Gregg J F, Jouguelet E, Ounadjela K, Petej I, Thompson S M and Thornton M J 2002 *J. Phys. D: Appl. Phys.* **35** 186
- [138] Rashba E I 2000 *Phys. Rev. B* **62** R16267
- [139] Schmidt G, Ferrand D, Molenkamp L W, Filip A T and van Wees B J 2000 *Phys. Rev. B* **62** 4790
- [140] Jonker B T and Flatté M *Nanomagnetism* 2006 ed Mills D L and Bland J C (Amsterdam: Elsevier)
- [141] Kikkawa J M, Smorchkova I P, Samarth N and Awschalom D D 1997 *Science* **277** 1284
- [142] Kikkawa J M and Awschalom D D 1999 *Nature* **397** 139
- [143] Naber W M, Faez S and van der Wiel W G 2007 *J. Phys. D: Appl. Phys.* **40** R205
- [144] Hueso L E, Pruneda J M, Ferrari V, Burnell G, Valdés-Herrera J P, Simons B, Littlewood P, Artacho E, Fert A and Mathur N 2007 *Nature* **445** 410
- [145] Awschalom D D, Flatté M E 2007 *Nature Phys.* **3** 153
- [146] Xu Y B and Thompson S M (ed) 2006 *Spintronic Materials and Technology* (London: Taylor and Francis) ISBN 0-8493-9299-3
- [147] Žutić I, Fabian J and Das Sarma S 2004 *Rev. Mod. Phys.* **76** 323
- [148] Barnaś J and Fert A 1998 *Phys. Rev. Lett.* **80** 1058
- [149] Majumdar K and Hershfield S 1998 *Phys. Rev. B* **57** 11521
- [150] Ono K, Shimada H and Ootuka Y 1998 *J. Phys. Soc. Japan* **67** 2852
- [151] Loss D and DiVincenzo D P 1998 *Phys. Rev. A* **57** 120
- [152] Kane B 1998 *Nature* **393** 133